A DYNAMIC ONE-DIMENSIONAL WATER QUALITY MODEL

by

P Huizinga

NATIONAL RESEARCH INSTITUTE FOR OCEANOLOGY
COUNCIL FOR SCIENTIFIC AND INDUSTRIAL RESEARCH

CSIR RESEARCH REPORT 562

Stellenbosch, South Africa
March 1985

A DYNAMIC ONE-DIMENSIONAL WATER QUALITY MODEL

by

P Huizinga

NATIONAL RESEARCH INSTITUTE FOR OCEANOLOGY
COUNCIL FOR SCIENTIFIC AND INDUSTRIAL RESEARCH

CSIR RESEARCH REPORT 562

Stellenbosch, South Africa
March 1985

ABSTRACT

Urban and industrial development is taking place around many estuaries in South Africa. As a consequence such actions as the release of domestic and industrial wastes into these estuaries or the reduction of freshwater inflow, often strongly affects their ecologies. Difficulty has been experienced in the prediction of the quantitative impact of these wastes on the water quality of the estuary as a whole.

To overcome this problem the one-dimensional dynamic water quality model presented in this report has been developed as a means of predicting transport and concentrations of pollutants or other constituents (for example, salinites) in estuaries. It can be operated at relatively low cost (a few hundred Rand) for long prototype periods (months).

It is operated in conjunction with a one-dimensional hydrodynamic model. Phenomena such as spring-neap-spring tidal variations, river floods and evaporation, which sometimes have considerable influence on the water quality can all be taken into account.

CONTENTS

CONTENTS (continued)

LIST OF FIGURES

FIGURE 13 Knysna model (Figure 11). Variation of concentrations with time at indicated positions. DW = 2.0 m^2/s.

FIGURE 14 Knysna model (Figure 11). Variation of concentrations with time at indicated positions. DW = 2.0 m^2/s.

FIGURE 15 Knysna model (Figure 11). Variation of concentrations with time at indicated positions. DW = 6.0 m^2/s.

FIGURE 16 Knysna model (Figure 11). Variation of concentrations with time at indicated positions. DW = 6.0 m^2/s.

FIGURE 17 Knysna model (Figure 11). Variation of concentrations with time at indicated positions. DW = 6.0 m^2/s.

FIGURE 18 Knysna model (Figure 11). Variation of concentrations with time at indicated positions. DW = 12.0 m^2/s.

FIGURE 19 Knysna model (Figure 11). Variation of concentrations with time at indicated positions. DW = 12.0 m^2/s.

FIGURE 20 Knysna model (Figure 11). Variation of concentrations with time at indicated positions. DW = 12.0 m^2/s.

FIGURE 21 Knysna model. Disbribution of concentrations at low water neaptide. DW = 2.0.

FIGURE 22 Knysna model. Distribution of concentrations at high water neaptide. DW = 2.0.

FIGURE 23 Knysna model. Distribution of concentrations at low-water springtide (at 760 hours). DW = 2.0.

FIGURE 24 Knysna model. Distribution of concentrations at high-water springtide (at 766 hours). DW = 2.0.

FIGURE 25 Knysna model. Longitudinal salinity profiles. Calibration of model on salinity distributions.

FIGURE 26 Knysna model. Longitudinal salinity profiles. Calibration of model on salinity distributions.

FIGURE 27 Knysna model. Influence of a 1:2 year river flood on salinity concentrations.

FIGURE 28 Knysna model. Influence of a 1:2 year river flood on salinity concentrations.

FIGURE 29 Knysna model. Salinities at indicated positions under different flow conditions (1.0; 0.5; 0.3 m^3/s)

FIGURE 30 Knysna model. Salinities at indicated positions under different flow conditions (1.0; 0.5; 0.3 m^3/s)

FIGURE 31 Knysna model. Salinities at indicated positions under different flow conditions (1.0; 0.5; 0.3 m^3/s)

FIGURE 32 Knysna model. Salinities in main channel at springtide under different flow conditions (1.0; 0.5; 0.3 m^3/s)

FIGURE 33 Knysna model. Salinities in main channel at neaptide under different flow conditions (1.0; 0.5; 0.3 m^3/s)

1. INTRODUCTION

The accurate modelling of water quality in rivers and estuaries requires a careful consideration of the processes involved and the limitations of various modelling techniques. Flows of water and transport and dispersion of pollutants in rivers and estuaries are governed by physical processes on macro- and microscales. Three-dimensional models with very fine resolution in space and time would be required to simulate these latter processes in detail. The areas under investigation (estuaries) are often extensive and associated problems almost always involve the study of the effects of pollutants over long periods (months, years).

A wide variety of mathematical models have been developed, such as those to study micro-processes for short periods and others for studying macro-processes for long periods. Most of these, however, have been developed to serve specific purposes and as such limitations exist to enable them to be operated on present day computers at reasonable computation times and expenses. For investigators it is very important to know the possibilities and limitations of a model to be used for a certain application.

Two- and three-dimensional time-dependent water quality models have been developed, but are often far too expensive to operate for periods of months or years. Steady-state models are also available but many influences like spring-neap-spring tidal fluctuations or irregular inflow of fresh river water are neglected in these models.

For the investigation of many estuaries a dynamic one-dimensional water quality model capable of modelling situations such as spring-neap-spring tidal variations and irregular river flow for long periods at reasonable costs would be very useful.

Such a model, which is operated in conjunction with a one-dimensional hydrodynamic model, is described in this report. It can be readily applied to any estuary if sufficient prototype data is available and easily copes with simulations for periods of several months or even a full year. The program has been written in such a way that a new model application can be done simply by supplying a new data set.

2. DYNAMIC ONE-DIMENSIONAL WATER QUALITY MODELS

One-dimensional advection and dispersion is described by the formula (see list of symbols):

$$\frac{\partial(Vol.C)}{\partial t} = \frac{\partial(Ax.K.\frac{\partial C}{\partial x})}{\partial x}.dx - \frac{\partial(Ax.U.C)}{\partial x}.dx \qquad (2\text{-}1)$$

Extra terms can be included for other phenomena such as breakdown and growth or lateral inflows of contaminants.

Computational schemes are often designed for a simplified version of this equation in which constant velocity, depth and cross-sectional area are assumed:

$$\frac{\partial C}{\partial t} + U\frac{\partial C}{\partial x} = K\frac{\partial^2 C}{\partial x^2} \qquad (2\text{-}2)$$

Mathematical models based on this formula (2-2) can give very good results if applied to channels and rivers with almost constant flow and cross-sectional area. They should not be applied to estuaries with irregular topography and under tidal influence.

A scheme based on the method of characteristics (Holly, Preissmann, 1977), which was developed for two-dimensional applications was also tested for one-dimensional situations. A sketch to explain the method is shown in Figure 1A. N and N+1 denote grid points at the two ends of a section at which concentrations (C_N, C_{N+1}) derivatives of concentrations with distance (CX_N, CX_{N+1}) and velocities (U_N, U_{N+1}) are known. At time level $t_o+\Delta t$, N^1 and $N+1^1$ are the given section ends, $U^1{}_N$ and $U^1{}_{N+1}$ are known (from hydrodynamic computations) and $C^1{}_N$, $C^1{}_{N+1}$, $CX^1{}_N$ and $CX^1{}_{N+1}$ have to be computed. Knowing the velocities (U) the path of a particle (or characteristic) which at $t_o+\Delta t$ arrives at $N+1^1$ can be estimated by

interpolation to have emanated from position A at time level t_o. Also knowing C_N, CX_N, C_{N+1} and CX_{N+1} an estimation can then be made for C_A and CX_A at A. Through advection C_A and CX_A are then transported without change to $N+1^1$. In a next step the effect of diffusion is also taken into account.

If the velocities (U) are constant with distance and time then the position A can be computed very accurately and the method will give very good results. However at variable velocities position A cannot be computed very accurately and the newly computed concentrations will then also become inaccurate. This method can, therefore, only be applied successfully to situations with almost constant flow and minor changes in topography between sections.

3. CONNECTED-CELLS MODEL

3.1 General

The computational method on which this model is based is similar in certain ways to that described by Orlob (1972). In principle it is based on a finite difference approximation of formula 2-1. Per timestep it consists of two stages. First, the total advective and diffusive transport between nodes are computed. In other words the right-hand side of formula 2-1 is computed. Then, knowing the change in volume in a node and also the in- and outflow volumes and concentrations, the new concentration for each node can be computed. Special routines are used to handle splitting points and positions where pollutants are released.

3.2 Advective Transport Computation (Figure 1B)

The advective transport through a cross-section during a time-step can be computed directly from the flow through that cross-section for that timestep multiplied by the average concentration. For section M-1 between nodes N-1 and N on Figure 1B this transport is:

$$ATR_{M-1} = Q_{M-1} \cdot C_{M-1} \cdot \Delta t$$

In the same way for section M:

$$ATR_{M} = Q_{M} \cdot C_{M} \cdot \Delta t \qquad (3-1)$$

If there are no splitting points at nodes N-1, N or N+1 a linear interpolation, together with a slight correction due to the velocity U, can be made to determine C_M:

$$C_M = C_N + (C_{N+1} - C_N) \cdot (0,5 \cdot dx_M - 0,5 \cdot U_M \cdot \Delta t)/dx_M \qquad (3-2)$$

and:

$$C_{M-1} = C_{N-1} + (C_N - C_{N-1}).(0,5.dx_{M-1} - 0,5.U_{M-1}.\Delta t)/dx_{M-1} \qquad (3-3)$$

At release positions and at splitting points (Figure 1C) sudden changes of concentrations can occur. For those situations other interpolation routines are used to estimate concentrations through cross-sections (C_M). If C_{N+1} is a splitting point and C_N is not, then C_M is determined by linear extrapolation from C_{N-1} and C_N. If this would cause negative values for C_M, then C_M is set equal to zero. If C_N and C_{N+1} are splitting points and the flow is to the right then C_M is taken to be equal to C_N.

3.3 Dispersive Transport Computation (Figure 1B)

Dispersion in estuaries is described extensively by many authors (see for example Fisher 1979), but concerning the main problem, which is the determination of the dispersion coefficient (K), it is said that no predictive formula that works in general exists. For a number of tests described in this report the coefficient was determined as suggested by Leendertse (1970). It is built up of a constant part and a part dependent on velocity, depth and Chezy-coefficient.

$$K = \frac{Df|U|.R}{Cf} + Dw \qquad (3-4)$$

In the salinity tests for the Knysna estuary the dispersion coefficient was determined from the salinity distribution in the estuary and the inflow of fresh water.

$$K = \frac{(\partial S/\partial x)}{(U_N).S} \qquad (3-5)$$

U_N results in the net downstream velocity caused by the fresh-water discharge.

The dispersive transport through a cross-section (Figure 1B) during a timestep (Δt) is computed by:

$$DTR_{M-1} = -K_{M-1}.(C_N - C_{N-1}).\Delta t.A_{M-1}/dx_{M-1} \qquad (3\text{-}6)$$

and

$$DTR_M = - K_M (C_{N+1} - C_N).\Delta t.A_M/dx_M \qquad (3\text{-}7)$$

3.4 Computation Of Concentrations

After having computed the transports through all the cross-sections and also knowing the changes in volumes for all the nodes, the next step is to compute the new concentrations for all the nodal points. CTR_N, the total transport though all the sections leading to nodal point N, is then used to compute the new concentration in node N.

$$C^1_N = (C_N.Vol_N + CTR_N)/Vol^1_N \qquad (3\text{-}8)$$

If N is also an inflow position (for example, from an outfall), the extra transport towards N due to this inflow is also included in CTR_N.

3.5 Stability And Accuracy

The water quality model is connected to an explicit one-dimensional hydrodynamic model (CSIR, 1976) and is being operated at the same schematization and timestep. This setup implies certain disadvantages but model simulations have shown that it is a practical combination.

For stability reasons the timestep of the hydrodynamic computation is limited due to the Courant criterion.

$$\Delta t \leq \frac{\Delta x}{\sqrt{gR}} \qquad (3\text{-}9)$$

For advective transport alone a similar criterion is valid for the water quality computation.

$$\Delta t < \frac{\Delta x}{U} \qquad (3\text{-}10)$$

The celerity of the long wave ($\sqrt{gR}$) is normally an order of magnitude faster than the water velocity; therefore, if both models are operated on the same timestep, the Courant criterion for the hydrodynamic model determines the timestep of the computation.

Normally the water level variation with time and distance is gradual, but variations of concentrations can be sudden with the result that the section lengths in the water quality model must be small.

Therefore, in this model combination the section length is selected first, based on the topography and on the accuracy wanted from the water quality computation and then the timestep is set, based on the Courant criterion for the hydrodynamic computation.

3.6 Adaption To Topography

The model has facilities to adapt cross-sectional areas, hydraulic radii, surface areas and volumes to raising and falling of water levels, which makes it particularly suitable for applications to tidal estuaries.

4. MODEL APPLICATIONS

4.1 General

Some results obtained with the model are presented here to give some impression of the model's capabilities as well as some of its limitations. Tests were done on theoretical channels with rectangular cross-sections. Results are also shown of applications to the Swartkops and Knysna estuaries.

4.2 Test Models

4.2.1 Channel with rectangular cross-section

The dimensions of the channel are:

depth	=	2 m	(to mean water level)
dx	=	200 m	(section length)
width	=	100 m	
length	=	15 400 m	(77 sections of 200 m)

At section 77 the channel is closed off while at section 1 an open boundary condition similar to an average tidal variation is applied according to:

$$H = 1{,}0 \sin(2\pi\, t/45000)$$

During the test the chezy coefficient for each section was computed at every timestep according to:

$$Cf = 37.5 + 18 \log R$$

The results of the water quality computations are presented in Figures 2A and 2C. In both tests an initial normal distribution of concentrations was assumed and the water quality computation was begun 16.5 hours after the start of the hydrodynamic computation.

On the right-hand side of the graphs the distributions are shown at high water at intervals of two tidal cycles and similar graphs of concentrations for low water at the same intervals are shown on the left. Figure 2A shows the results for a test with only advective transport included in the computation, indicating that because of the minor changes in the concentrations the numerical diffusion is very small.

In the test displayed in Figure 2C diffusive transport was also included in the computation with fairly typical values for DW = 6.0 and Df = 18.48 assumed for the constants of formula 3-4. Comparison of Figures 2A and 2C indicates that numerical diffusion is negligible.

4.2.2 Channel with branching

The total length of the channel is the same as that of the previous test model, but between nodes 40 and 46 (of the previous test) the single channel has been split up into several branches as shown in Figure 3. The total width of these branches was still the same, 100 m; for instance section 40, 48 and 56 are each 33.33 m wide. The same two tests were repeated with this test model and the results are shown in Figures 2B and 2D. Comparison of Figures 2A and 2B show that the numerical diffusion is slightly stronger in the branched channel, but still very small when normal diffusion is included in the computation (Figures 2C and 2D).

4.2.3 Channel with constriction

In this test model the channel length was increased to 90 sections of 200 m with a total length of 18 000 m, but with a constriction in the channel as shown in Figure 4.

The same hydrodynamic conditions were applied as described in 4.2.1.

Figure 5A gives the results of a computation with only advective transport, and Figures 5B and 5C are from tests with DW = 2.0 and DW = 6.0 respectively (see formula 3-4). In both cases Df = 18.48 was used.

The numerical diffusion (Figure 5A) is small again compared to diffusion conditions the results of which are shown in Figures 5B and 5C.

4.2.4 Influence of Df

In the past simulations were done with high values (63.34) and low values (18.48) for Df. Therefore the influence of these values was investigated in this model test.

The same channel was used as described under Section 4.2.1 with 77 sections and a total length of 15 400 m, but the influence of a high and a low value for Df (formula 3-4) was tested.

The conditions were:

Figure 6A : DW = 0.0 Df = 18.48
Figure 6B : DW = 0.0 Df = 63.33

Comparison of Figures 6A and 6B shows that the influence of the value for Df is significant but not dramatically so. In model applications however one should be aware of this influence and try to use an optimal value for this constant that most closely represents the prototype diffusion.

4.3 Swartkops Estuary Model

4.3.1 General

The Swartkops river estuary, about 20 km east of Port Elizabeth on the south coast of South Africa, is in an area with many industrial and urban developments. An early version of the one-dimensional hydrodynamic model was applied to this estuary.

Subsequently a water quality model was made for this estuary. Some tests were done which show the potential of the model. A schematization is given in Figure 7F.

At node 1 a springtide water level variation with an amplitude of 0.81 m and a period of 12 hours was used for the open boundary condition. Different river flow conditions were assumed at section 69 at the upstream end of the model.

4.3.2 Effect of river flood on salinity

In this test a starting concentration of 9 000 units of a conservative pollutant (for example, salinity), was assumed for all the nodes. A minor river flood with a constant flow of 10 m^3/s was assumed to last for 24 hours. In Figure 8E the pollutant distributions are shown at intervals of 3 hours during this flood. After 24 hours the river flow was stopped and only tidal motions were present during the rest of the computation. The influence of the tide on the concentrations at a number of positions is visible in Figures 7A, 7B, 7C, 7D and 7E where the variations with time are plotted. In Figure 8A graphs are plotted of the concentrations in the estuary at 24, 240, 480 and 720 hours, indicating how the gradients of the concentrations smooth out with time in the estuary. Figures 8B, 8C and 8D show the changes over half a tidal cycle at different periods.

4.3.3 Effect of evaporation and low river flow on the distribution of concentrations

The same starting condition for concentrations was assumed as in the previous test but now a small constant riverflow of 0.5 m^3/s and an evaporation rate of 0.156 M/month was assumed. The effects of both are visible on the graphs of Figure 9, showing the distributions at different times during the simulation.

Figure 10 shows measured salinities (McLachlan, 1972). Both figures show the lower concentrations on the upstream end of the estuary and in the middle at dry periods higher concentration than sea salinity.

If enough river flow and evaporation data were available it would be possible to calibrate the model on the salinity data. This calibrated model could then be used to simulate the continuous change in salinity for the estuary.

4.4 Knysna Estuary Model

4.4.1 General

The Knysna estuary on the Cape south coast has a much more complicated channel system than the Swartkops estuary. A data set was prepared for a mathematical model of this estuary, and the schematization is given in Figure 11.

Two different test series were done with the Knysna model. In the first series all the model simulations were done for a constant inflow of conservative pollutant (for example, from an outfall). Later on field data was obtained of salinities in the estuary and a second series of model simulations for salinity distributions gave close similarity to the new prototype data.

4.4.2 Tests with constant inflow of conservative pollutant

4.4.2.1 Hydrodynamic conditions

A sinusoidal water level variation was applied as an open boundary condition at node 1. The amplitude followed a spring-neap-spring variation and the same graph of the water level variation is shown at the bottom of Figures 12 to 20. Further details are:

at springtide	:	ampl. = 0.875 m
at neaptide	:	ampl. = 0.325 m
open boundary (node 1)	:	$H = 0.045 + \text{ampl.} \sin(\frac{2\pi t}{T})$
tidal period	:	T = 45 000 (s)
chezy coefficient	:	Cf = 37.5 + 18 log R

At the upstream end of the model (section 33) a constant river-flow of 0.5 m^3/s was used as the other open boundary condition.

4.4.2.2 Conditions for the water quality computation

Some conditions were the same for all the tests:

a) Concentrations are computed in units per m^3 for a conservative constituent (no growth or breakdown).

b) Starting concentrations of 40 units/m^3 were assumed for the whole estuary. The purpose was to achieve a stabilized distribution in a relatively short time.

c) The inflow of pollutant began 12.5 hours after the start of the hydrodynamic computation to allow a "running-in" period for the hydrodynamic model. The release position is marked by R.P. on Figure 11.

d) A constant inflow of 0.0296 m^3/s with a concentration of 10^5 units/m^3 was maintained. This inflow corresponds with a daily inflow of 2 556 m^3 which was estimated for 1 990 by the Knysna Municipality (see also CSIR report C/SEA 7609).

e) All tests were done with Df = 18.48 (formula 3-4) and different values for Dw of 2.0, 6.0 and 12.0 m^2/s were used.

f) The computation results are presented in two ways, namely as time histories of concentrations at certain nodes (Figures 12 to 20) and as situation plots over the whole area (Figures 21 to 24).

4.4.2.3 Test 1, DW = 2.0 m^2/s

Time histories of the concentrations for ten locations are shown on Figures 12 to 14. Comparison with the water level variation at the bottom of these figures show very clearly the influence of the spring-neap-spring variation on the results, indicating that this variation is essential for any model tests for the Knysna estuary.

For all positions except those in the far upstream end of the estuary (25, 26 and 32) a build-up of concentrations is noticeable during and after neaptide when the exchange of pollutant with the open sea is at its least and a reduction of concentrations is noticeable during and shortly after springtide when the exchange with the open sea is at its greatest. The variation in concentration over a tidal cycle is, for most positions, also greatest during springtide and least during neaptide.

At Position 11 (Figure 12B) sharp double peaks are visible in the concentration graphs over each tidal cycle, just after neaptide. The explanation is that at these times two areas (patches) of high concentration are moving up and down the main channel and both are passing Position 11 during a tidal cycle.

Situation plots of the pollutants for the whole estuary at high and low water both at springtide and neaptide are shown in Figures 21 to 24. Two important features should be noticed, firstly the inflow of unpolluted sea water at high water over a long distance, especially at springtide and secondly the location of the release position causes very high concentrations behind Paarden island, caused by the very small volumes of water existing here at low tide.

4.4.2.4 Test 2, DW = 6.0 m^2/s (Figures 15 to 17)

Again the strong influence of the spring-neap-spring tidal variation on the concentrations is visible on all the graphs. The influence of the higher value for DW is strong at the nodes near the release positions (nodes 35, 39 and 43) where concentrations are significantly lower, while more upstream in the estuary the concentrations are slightly higher, compared with test 1.

4.4.2.5 Test 3, DW = 12.0 m^2/s (Figures 18 to 20)

The same tendency, already visible from tests 1 and 2 is visible in these results. The concentrations near the release position have lowered further, but those further upstream in the estuary have increased slightly more.

4.4.3 Tests on salinity distributions in the Knysna Estuary

4.4.3.1 General

Increasing demands for fresh water have led to investigations of the possibilities of extracting water from the Knysna river upstream of the estuary. It is important to know what effect this could have on the salinity distributions and variations and thus on the ecology of the estuary. Salinity concentrations were measured on a certain day, then the river flow was monitored for a period of about seven days then the salinities were measured again. An estimation was made for the dispersion coefficients in the estuary. With these data available, model simulations were done. The starting conditions were the salinity distributions of the beginning of a period. At the open sea boundary a recorded tidal variation was used and at the upstream end the recorded river flow was used for boundary conditions. The salinities computed with the model after the period were then compared with the measured salinities of the corresponding line. A re-assessment was then made of the dispersion coefficients and the model simulation was repeated. After a few tests good

agreement was achieved between model results and prototype data and the model was considered to be calibrated. Verification runs were done for other periods with equally good results. A number of model tests were then done under different flow conditions for investigating salinity distributions under these circumstances.

4.4.3.2 Calibration tests

In Figure 25A the start condition is shown, which was measured at low water on 18 January 1984 and which was used for the calibration runs. The period covered by the tests was from 18 till 25 January 1984. The river flow was constant at 0.8 m^3/s and at the open sea boundary the water level variation was recorded. A first estimation of the dispersion coefficient (K) was made using formula 3-5. In the first calibration test K = 45 m^2/s was used for all the sections. The model results are compared in Figure 25B for 25 January 1984. The model results are slightly higher compared to the field data in the upstream end (Sections 23-33) of the estuary.

A second calibration test was done in which K = 45 for all sections except K = 35 for Sections 23-26 and K = 25 for Sections 27-32. The model results are now slightly too low at the upstream end of the estuary indicating that the adaptation was a little too drastic (Figure 25C).

A third calibration test was therefore done in which K = 45 for all sections except K = 40 for Sections 23--26 and K = 35 for Sections 27-32. Figure 25D shows that excellent agreement between model results and field data was achieved. In all further tests the same dispersion coefficients were used.

4.4.3.3 Verification tests

The first verification test was done for the period 10-17 March 1984. The flow was variable from 1.82 m^3/s on 10/03/1984 to 2.90 m^3/s on 13/03/1984 to 1.15 m^3/s on 17/03/1984. The agreement between model results and prototype data was still good for 17/03/1984, especially if one considers that the river flow data was probably not very accurate (Figure 26B).

A second verification test was done for the period 16-23 April 1984. The flow data used was 0.85 m^3/s for 16-19/04/1984, 0.70 m^3/s for 20 and 21 April 1984 and 0.60 m^3/s for 22 and 23 April 1984. The results again show good agreement between model and prototype results (Figure 26D).

4.4.3.4 River flood test

In Figures 27 and 28 the effect of a minor river flood on the salinities in the estuary is shown. The shape of the hydrograph with a maximum flow of 40 m^3/s is shown on each graph of Figure 27. The initial salinity concentrations in this test were the same as those used in the calibration test (4.4.3.2) and are indicated in Figure 25A. At the upstream end of the estuary, positions E and F (see also Figure 11), the salinities drop down to zero but later return to their normal values. The graphs for positions A, B, C and D all show the effects of this flood, with the strongest influence upstream in the estuary and the weakest effect near the estuary month. On all the graphs the effect of the spring-neap-spring tidal variation is also visible. In Figure 28A, shortly after the maximum flow, the distributions of the salinities in the estuary is shown at hourly intervals. Figures 28B and C show the salinity distributions at 3-day intervals at low water and at high water respectively. As a result of dispersion the concentrations increase again after the flood.

4.4.3.5 Tests under different constant-flow conditions (1.0, 0.5 and 0.3 m^3/s)

The start condition in all these tests was the salinity distributions as measured at low water on 18 January 1984. The results are shown as time-histories of salinities at the positions A, B, C, D, E and F (Figures 29, 30 and 31) and as graphs of distributions in the main channel of the estuary in Figures 32 and 33.

At position A (Figure 29) the results look very similar for the three flow conditions. The salinities are almost equal to the sea salinities.

At position B (Figure 29) the graphs indicate slightly too low starting conditions for all three flow conditions, but the model adapts itself fast and all three graphs show that concentrations become close to sea salinities.

The same tendencies are visible for position C (Figure 30).

The graphs for position D (Figure 30) show more definition, due to the tidal influence and also of the spring-neap-spring variation.

This tendency is even stronger for positions E and F (Figure 31) and these graphs also show that the average concentrations decrease with increasing flow.

In Figure 32 graphs of salinity distributions in the main channel at springtide at high water and at low water are plotted for the three different flow conditions. Similar graphs for a neaptide situation are plotted on Figure 33. For Sections 1-22 all the graphs show little difference between high and low water, but considerably bigger differences for Sections 23-33, in the narrow upper channel of the estuary. It can also be seen that the influence of the fresh water inflow is considerable at the upper end of the estuary, but small in the downstream part (Section 1-22).

4.4.4 Details of computation

The Knysna model tests were done at a timestep of 30 seconds to fulfil the Courant criterion for the hydrodynamic computation (formula 3-8). As stated before (section 3.5) the hydrodynamic and water quality computations were done at the same timestep. The operation of the Knysna model on the CDC-cyber 750 computer could be done at a cost of about R10 a day (prototype time).

5. CONCLUSIONS

A one-dimensional model which is 100 per cent conservative is presented in the report. Simulations with test models of simple geometrical structure show that the numerical dispersion is very small. This numerical dispersion increases slightly in models with irregular topography and networks, but for the test cases described here this dispersion was always very small.

The model can be easily applied to suitable estuaries, that is, estuaries that are vertically well-mixed and in which two-dimensional horizontal current patterns are negligible. The applications of the model to the Swartkops and Knysna estuaries show this feature.

The calibration and verification runs for the Knysna estuary especially show the reliability of the model. The subsequent tests for different flow conditions show the potential of the model as a means of investigating the influence of these conditions on salinities, and these results can be used for further ecological studies.

The model could be developed further to simulate chemical and biological processes, but it would probably be better to use other existing models, like the Dynamic Estuary Model (DEM) from the Environmental Protection Agency (EPA) in the USA. As mentioned before, the model presented here has features similar to those of this DEM.

Finally, the present combination of the hydro-dynamical with the water-quality model computations has the disadvantage that the model has to be operated on a small section length (100-500 m) and timestep (30-60 seconds). It was possible, however, to carry out the tests at relatively low cost. The Knysna model, for example, was operated at about R10 per day or R300 per month. This shows that the model can be a practical tool for many investigations at reasonable cost.

ACKNOWLEDGEMENT

Special acknowledgement is made for contributions by the late Mr Peter Haw who, as a post-graduate student at the School of Environmental Studies at Cape Town University, conducted extensive studies of the salinity distributions in the Knysna estuary. Many fruitfull discussions were held with him on the modelling techniques and he also collected excellent prototype data which was used for the model calibration.

REFERENCES

HOLLY, F.M. and PREISSMANN, A. Accurate Calculation of Transport in Two Dimensions. ASCE, Journal of the Hydraulics Division, Nov. 1977.

ORLOB, G.T. Mathematical Modelling of Estuarial Systems. International Symposium on Modelling Techniques in Water Resources Systems, Ottawa, 1972.

McLACHLAN, A. Studies on burrowing bivalues in the Swartkops Estuary. M.Sc Thesis, University of Port Elizabeth, 1972.

FISHER, H.B., LIST, E.J., KOH, R.C.Y., IMBERGER, J. and BROOKS, N.H. Mixing in Inland and Coastal Waters, New York, 1979.

LEENDERTSE, J.J. A water-Quality Simulation Model for Well-Mixed Estuaries and Coastal Seas: Volume I, Principles of Computation. RM-6230-RC, February 1970.

CSIR (1976). Saldanha Bay, the assessment of field data, the mathematical model and the physical model, Volume II. CSIR Report C/SEA 7620/2, December 1976.

LIST OF SYMBOLS

ATR	=	advective transport
A_X, A_N	=	cross-sectional area at x or N (m^2)
C	=	concentration (kg/m^3)
C_N	=	concentration of position N (kg/m^3)
CX_N	=	$\frac{\partial C}{\partial x}$ at position N
Cf	=	chezy coefficient ($m^1/_2/s$)
CTR	=	sum of all advective and dispersive transport to and from a nodal position
Df	=	constant used in the formula for the dispersion coefficient (3-4)
DTR	=	dispersive transport
DW	=	dispersion coefficient (m^2/s)
dx_N, dx_M	=	nodal length at N, section length at M (m)
g	=	acceleration due to gravity
H_N	=	water level to mean sea level (MSL) at node N(m)
K	=	dispersion coefficient (m^2/s)
M	=	identification of section number (also as subscript)
N	=	identification of nodal number (also as subscript)
Q, Q_M	=	flow through cross-section (M) (m^3/s)
R	=	hydraulic radius (m)
S	=	salinity concentration (mg/l)
t	=	time (s)
Δt	=	timestep of computation (s)
U	=	mean velocity (m/s)
U_M	=	mean velocity at section M (m/s)
U_N	=	net downstream velocity due to fresh-water discharge
Vol	=	volume (m^3)
x	=	distance (m)
^{1}	=	all variables marked like this are on a new time level

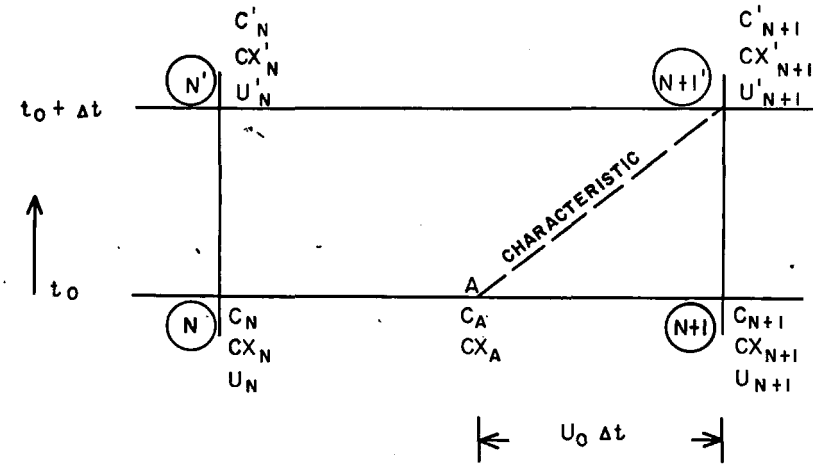

A. SCHEMATIZATION HOLLY-PREISSMANN SCHEME

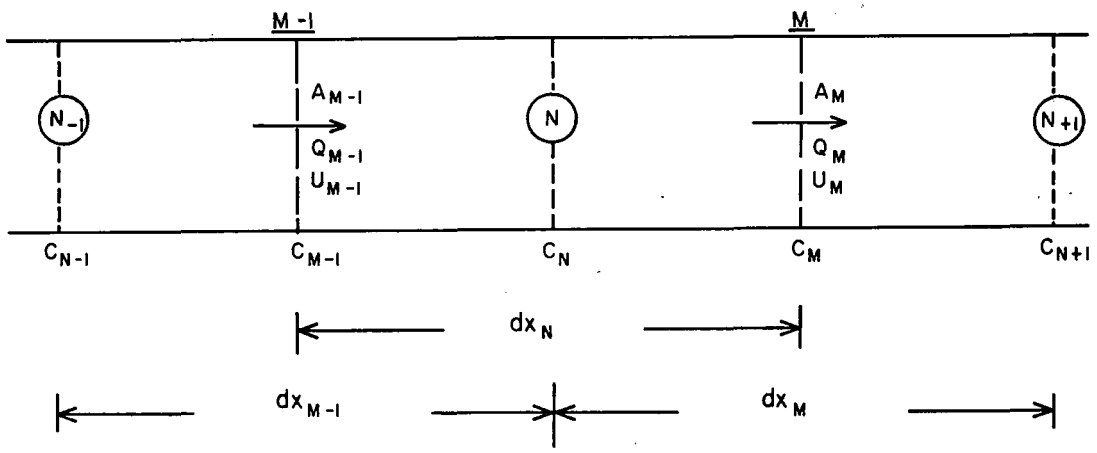

B. SCHEMATIZATION TRANSPORT COMPUTATION

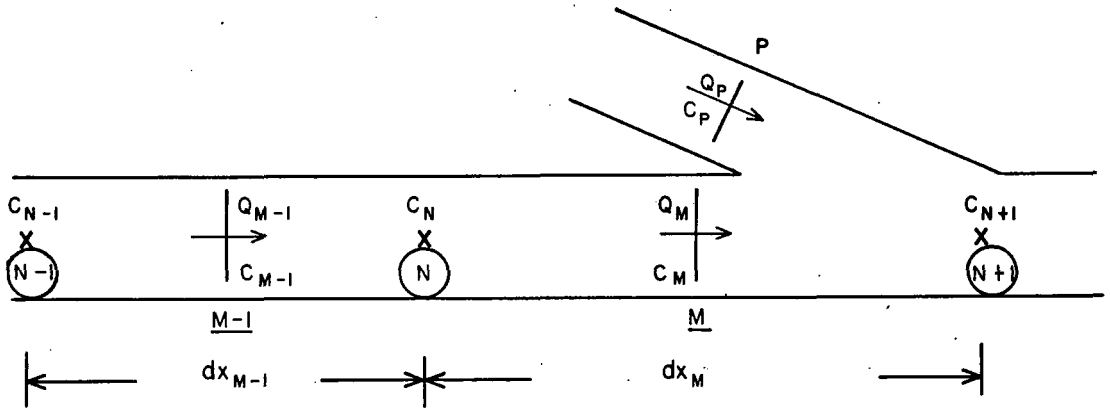

C. SCHEMATIZATION TRANSPORT COMPUTATION AT SPLITTING POINT

TRACED JBT CHECKED: DATE: REF.	1-DIMENSIONAL WATER-QUALITY MODEL SCHEMATIZATION OF COMPUTATIONAL SYSTEMS FOR ONE-DIMENSIONAL WATER QUALITY MODELS	FIGURE 1

NATIONAL RESEARCH INSTITUTE FOR OCEANOLOGY

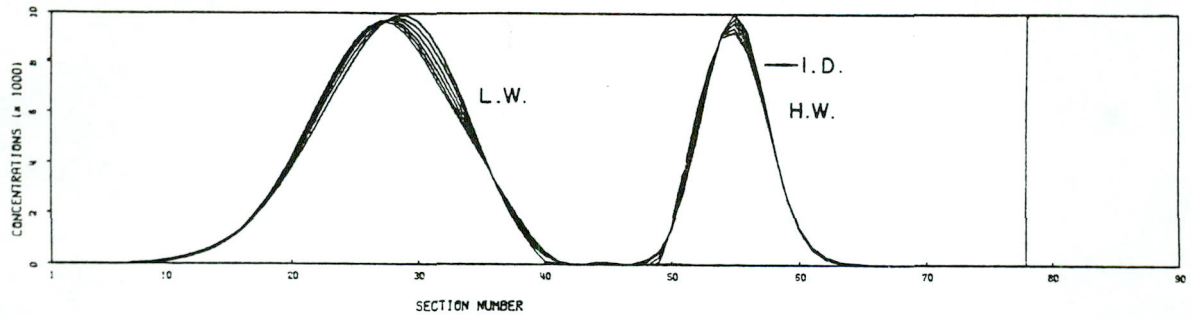

A. SINGLE CHANNEL ONLY ADVECTIVE TRANSPORT

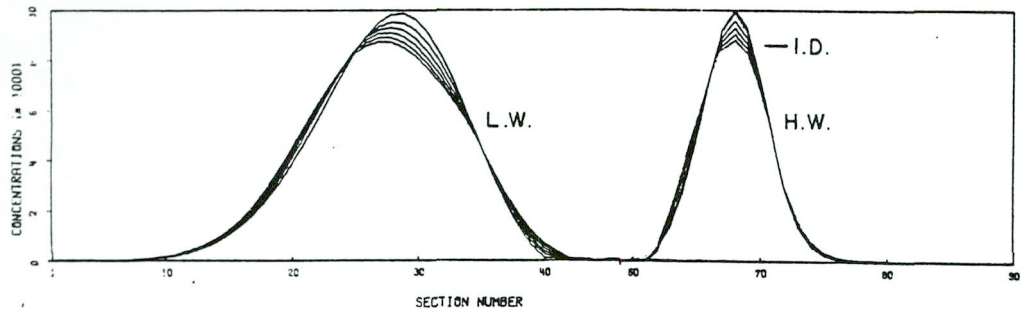

B. BRANCHED CHANNEL ONLY ADVECTIVE TRANSPORT

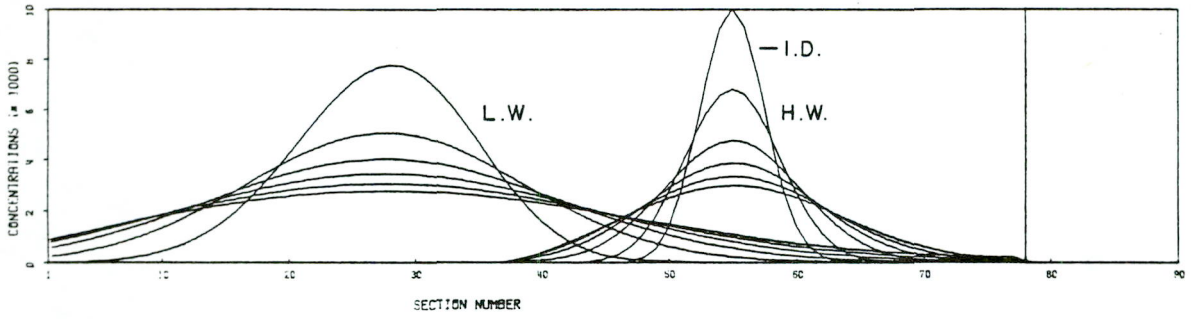

C. SINGLE CHANNEL DW = 6.0

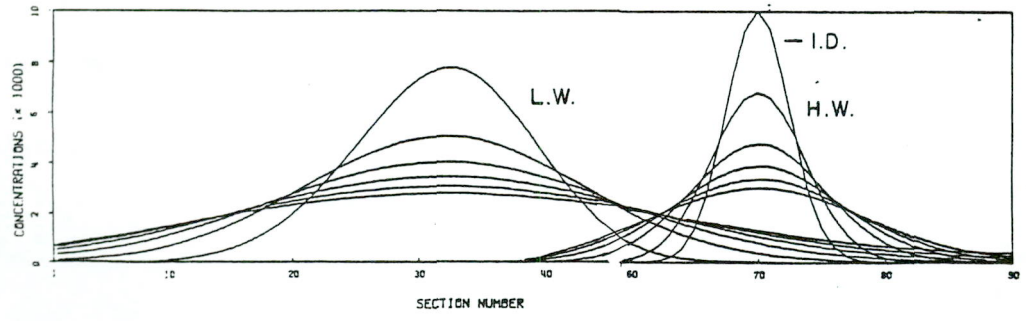

D. BRANCHED CHANNEL DW = 6.0

HYDRODYNAMIC : OPEN BOUNDARY AT NODE (1)
COMPUTATION CLOSED " " " (77) FOR SINGLE CHANNEL
" " " " (90) " BRANCHED "

WATER QUALITY : START COMPUTATION AT H.W. AT 16.5 HOURS
COMPUTATION WITH NORMAL DISTRIBUTION

H.W. HIGH WATER
L.W. LOW WATER
I.D. INITIAL DISTRIBUTION

TRACED: JBT CHECKED: DATE REF.	1-DIMENSIONAL WATER-QUALITY MODEL DISPERSION TESTS UNDER TIDAL INFLUENCE. DISTRIBUTIONS AT H.W. AFTER 16.5,29,54,79,104,129 HOURS AND AT L.W. AFTER 24,49,74,99,124,149 HOURS.	FIGURE 2

TRACED: JBT
CHECKED:
DATE:
REF:

1-DIMENSIONAL WATER-QUALITY MODEL

SCHEMATIZATION OF BRANCHED CHANNEL COMPARED WITH THAT OF SINGLE CHANNEL

FIGURE 3

NATIONAL RESEARCH INSTITUTE FOR OCEANOLOGY

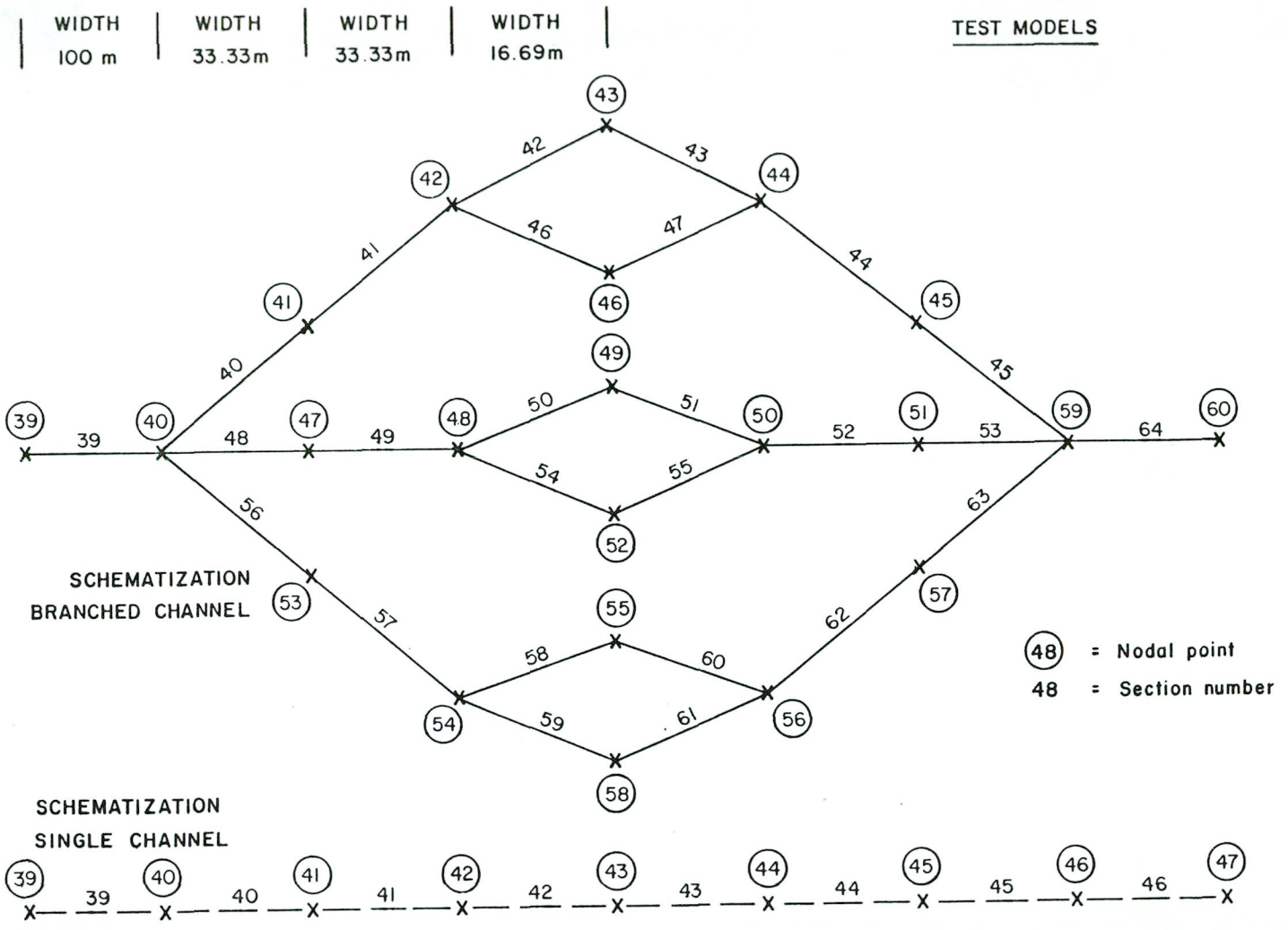

TRACED JBT
CHECKED
DATE
REF.

1-DIMENSIONAL WATER-QUALITY MODEL

LAYOUT OF A CHANNEL WITH A CONSTRICTION
MAXIMUM EBB AND FLOOD VELOCITIES ARE INDICATED

FIGURE 4

NATIONAL RESEARCH INSTITUTE FOR OCEANOLOGY

MAXIMUM POSITIVE VELOCITIES (m/s)

(⟶)

V =	.46	.53	.82	1.13	1.15	1.17	1.19	.88	.57	.48	.47

MAXIMUM NEGATIVE VELOCITIES (m/s)

(⟵)

V =	-.35	-.40	-.61	-.82	-.80	-.78	-.76	-.55	-.35	-.29	-.28

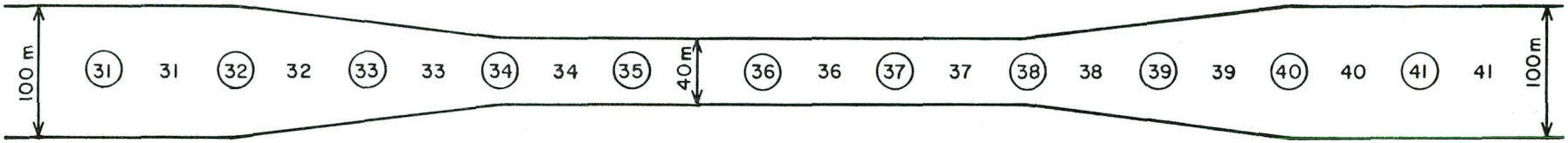

O =	20000	19250	14000	8750	8000	8000	8000	8750	14000	19250	20000
Vol =	(at O)	38500	28000	17500	16000	16000	16000	17500	28000	38500	40000

A =	(-1)	100	85	55	40	40	40	40	55	85	100	100
	(0)	200	170	110	80	80	80	80	110	170	200	200
	(+1)	300	255	165	120	120	120	120	165	255	300	300
	(+2)	400	340	220	160	160	160	160	220	340	400	400

DEPTH : MSL − 2.0 m

OPEN BOUNDARY AT SECTION (1), CONDITION : $H = 0.0 + 1.0 \sin\left(2\pi \frac{t}{45\,000}\right)$

CLOSED BOUNDARY AT SECTION (90)

SECTION LENGTH : 200 m

(34) = NUMBER NODAL POINT

33 = SECTION NUMBER

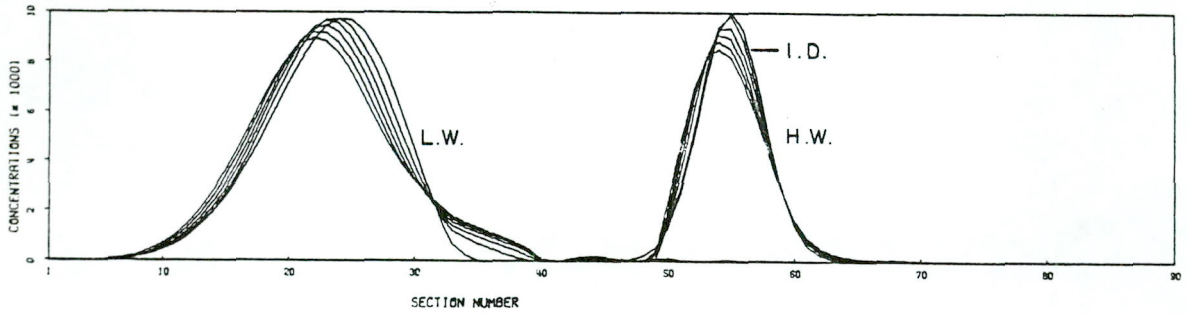

A. ONLY ADVECTIVE TRANSPORT

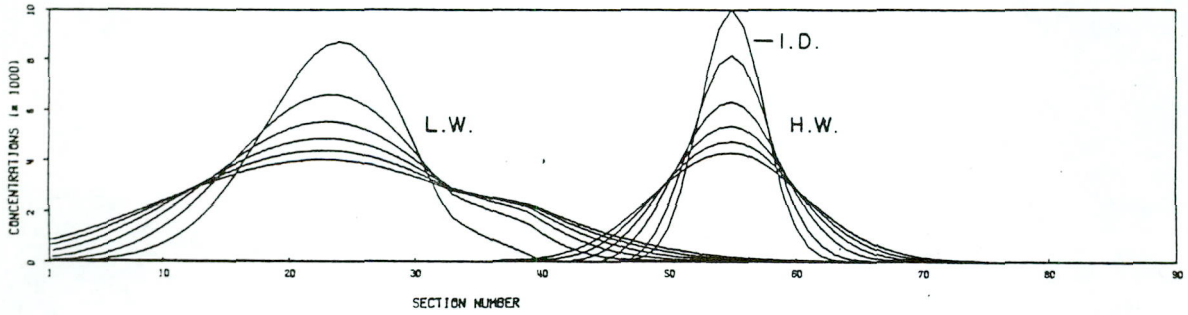

B. DW = 2.0

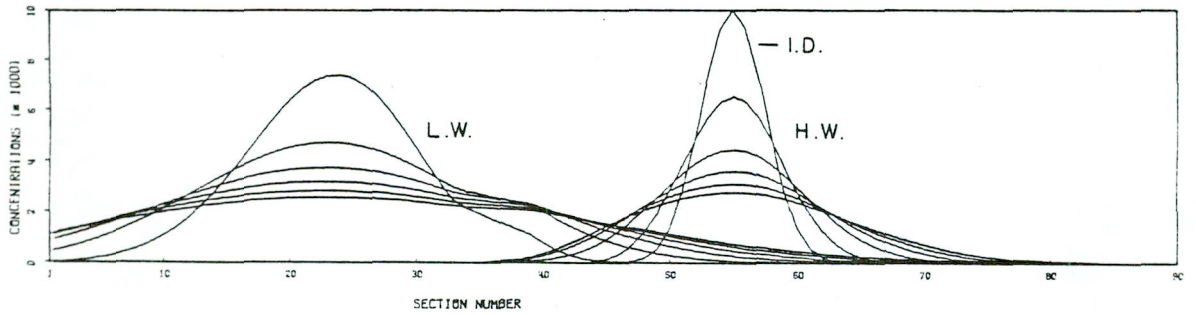

C. DW = 6.0

HYDRODYNAMIC : OPEN BOUNDARY AT NODE (1)
COMPUTATION CLOSED " " " (90)
CONSTRICTION IN CHANNEL (FIG 4)
WATER QUALITY : START COMPUTATION AT 16.5 HOURS
COMPUTATION WITH NORMAL DISTRIBUTION

H.W = HIGH WATER
L.W.= LOW WATER
I.D.= INITIAL DISTRIBUTION

TRACED JBT CHECKED DATE REF	1-DIMENSIONAL WATER-QUALITY MODEL DISPERSION TESTS UNDER TIDAL INFLUENCES FOR CHANNEL WITH A CONSTRICTION	FIGURE 5

NATIONAL RESEARCH INSTITUTE FOR OCEANOLOGY

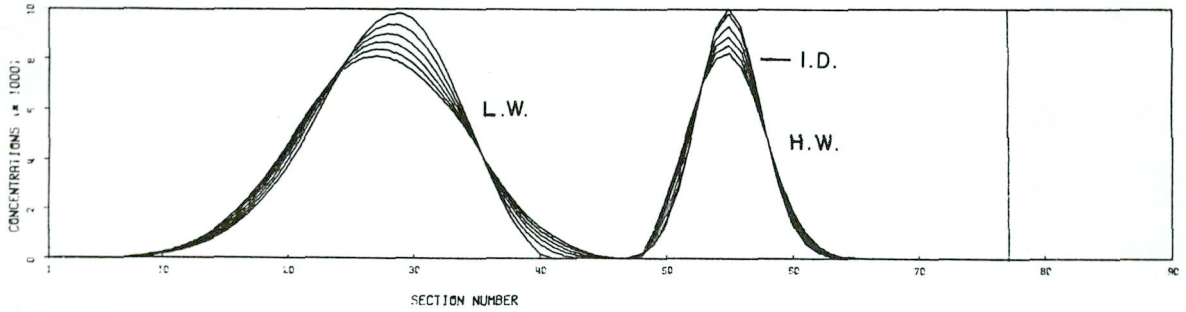

A. Df = 18.48 DW = 0.0

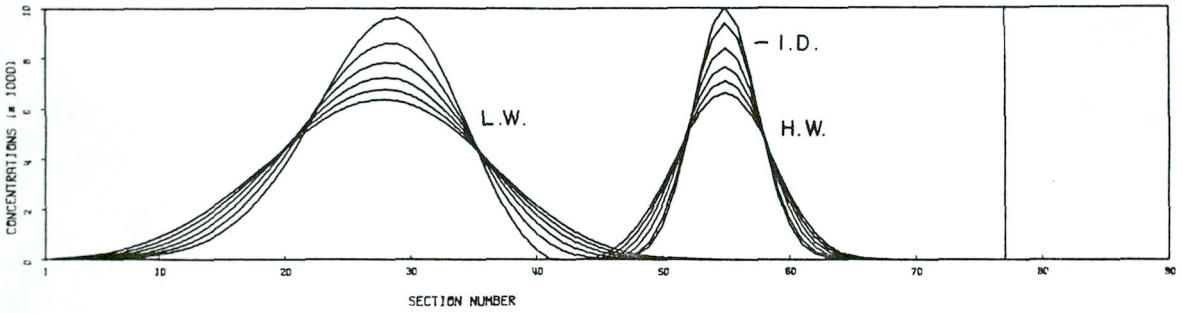

B. Df = 63.34 DW = 0.0

HYDRODYNAMIC : OPEN BOUNDARY AT NODE (1)
COMPUTATION CLOSED " " " (77)

WATER QUALITY : START COMPUTATION AT 16.5 HOURS
COMPUTATION WITH NORMAL DISTRIBUTION

H.W. = HIGH WATER
L.W. = LOW WATER
I.D. = INITIAL DISTRIBUTION

TRACED JBT CHECKED DATE REF	1-DIMENSIONAL WATER-QUALITY MODEL DISPERSION TESTS UNDER TIDAL INFLUENCES. EFFECT OF DF IN FORMULA 3-4 ON COMPUTATION RESULTS	FIGURE 6

NATIONAL RESEARCH INSTITUTE FOR OCEANOLOGY

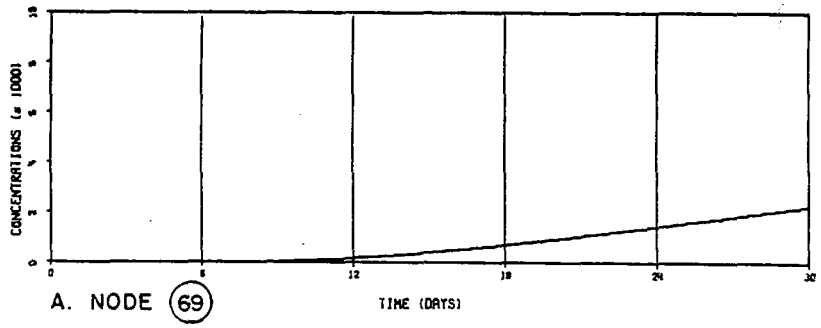

A. NODE (69)

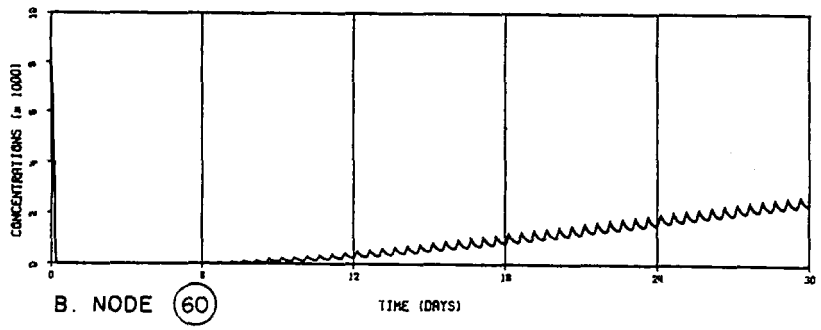

B. NODE (60)

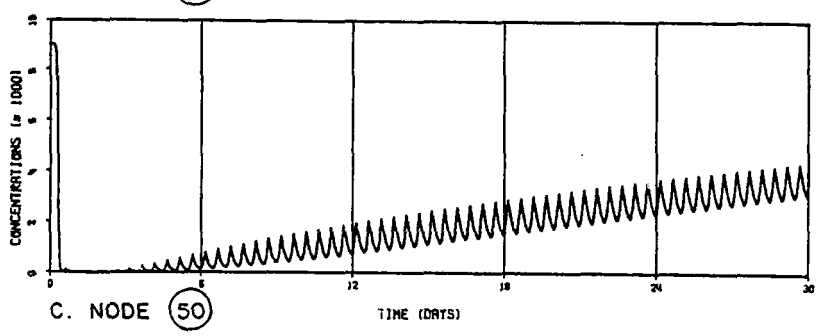

C. NODE (50)

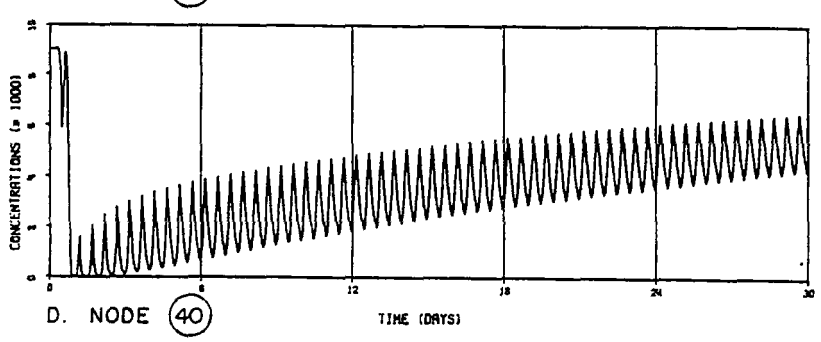

D. NODE (40)

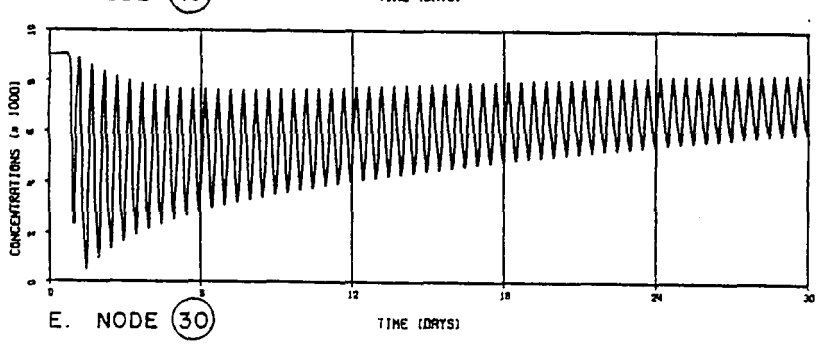

E. NODE (30)

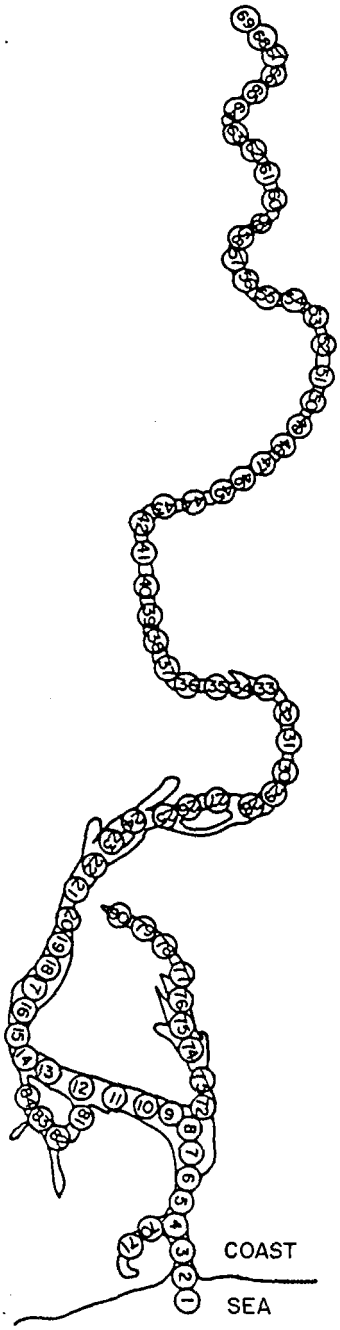

F. SWARTKOPS MODEL
SCHEMATIZATION
SECTION LENGTH = 250 m

NOTES:

RIVER FLOW 0 - 24 HOURS : 10 m^3/s
24 -720 " : 0 m^3/s
EVAPORATION : 0,156 m/month
DW : 6.0 m^2/s

TRACED JBT CHECKED DATE REF.	1-DIMENSIONAL WATER-QUALITY MODEL SWARTKOPS MODEL, CONCENTRATION AT FIVE POSITIONS DURING RIVERFLOOD (1-DAY) AND RECOVERY PERIOD (29 DAYS) AFTERWARDS	FIGURE 7

NATIONAL RESEARCH INSTITUTE FOR OCEANOLOGY

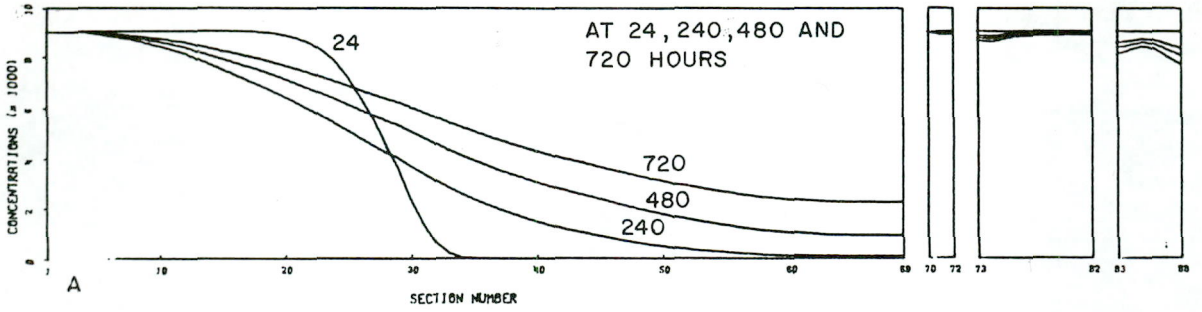

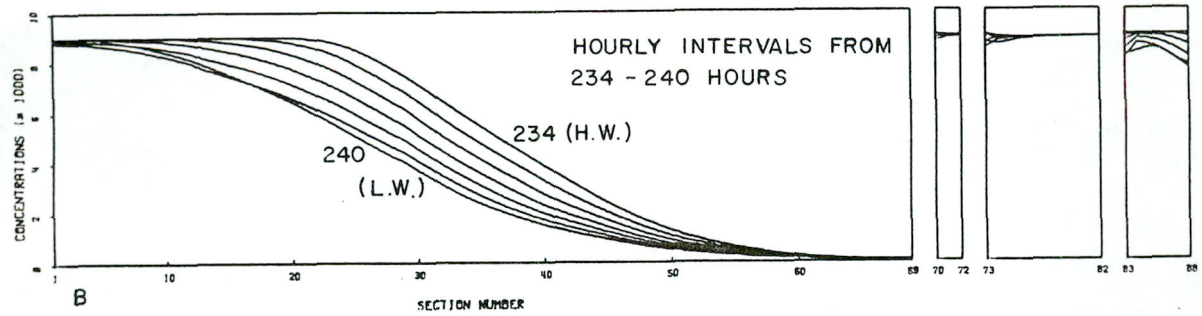

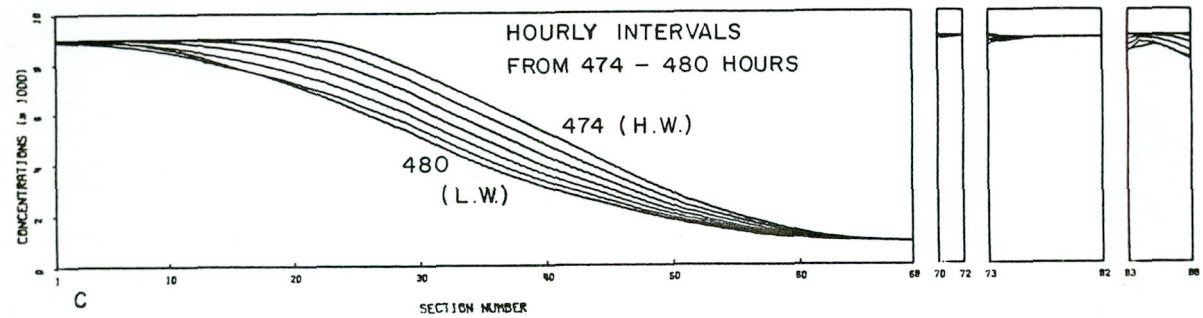

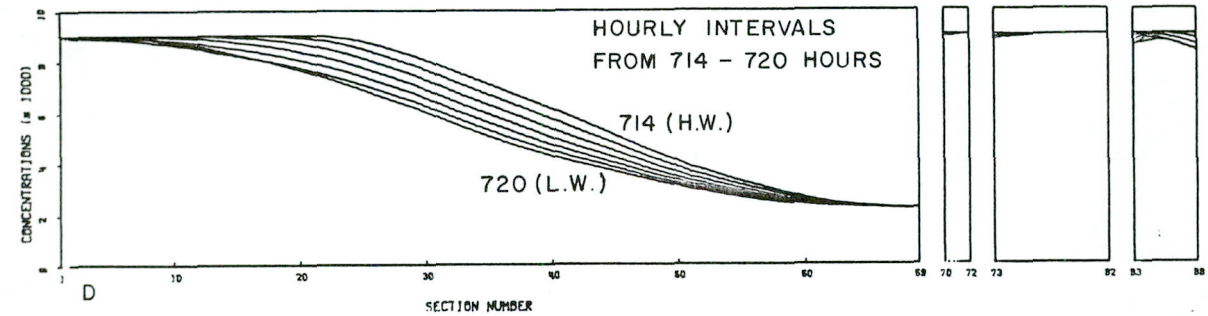

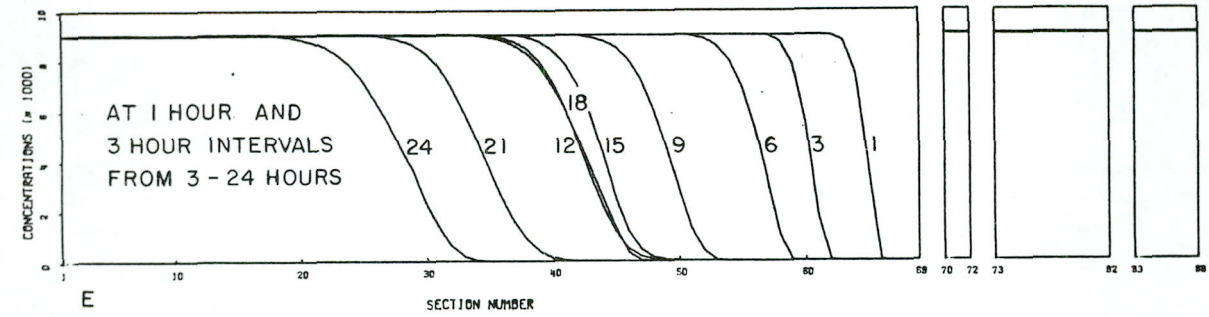

TRACED: JBT CHECKED DATE REF	1-DIMENSIONAL WATER-QUALITY MODEL SWARTKOPS MODEL CONCENTRATION PROFILES AT INDICATED HOURS IN MODEL DURING FLOOD TEST (SEE ALSO FIGURE 7)	FIGURE 8

NATIONAL RESEARCH INSTITUTE FOR OCEANOLOGY

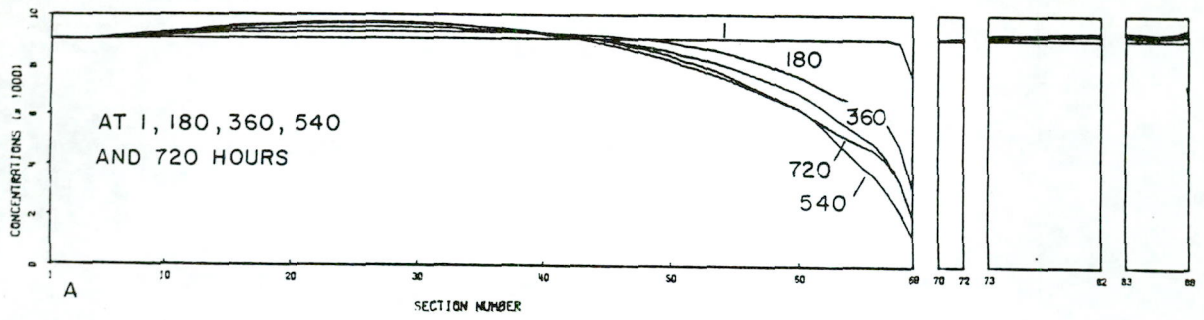

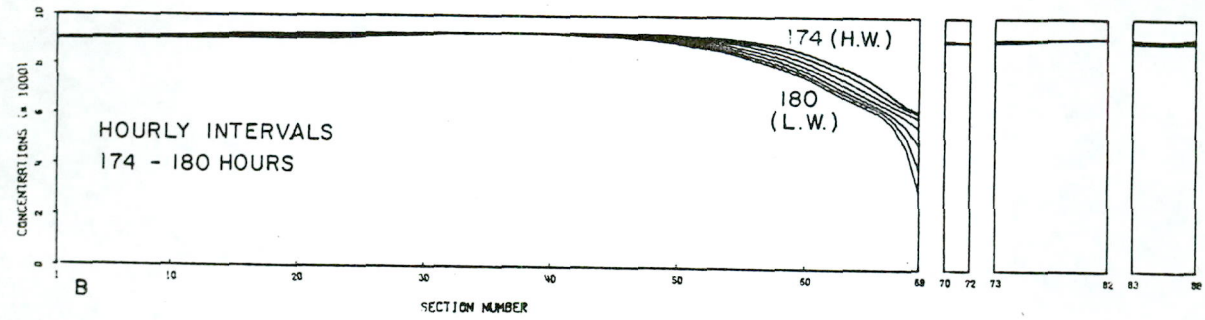

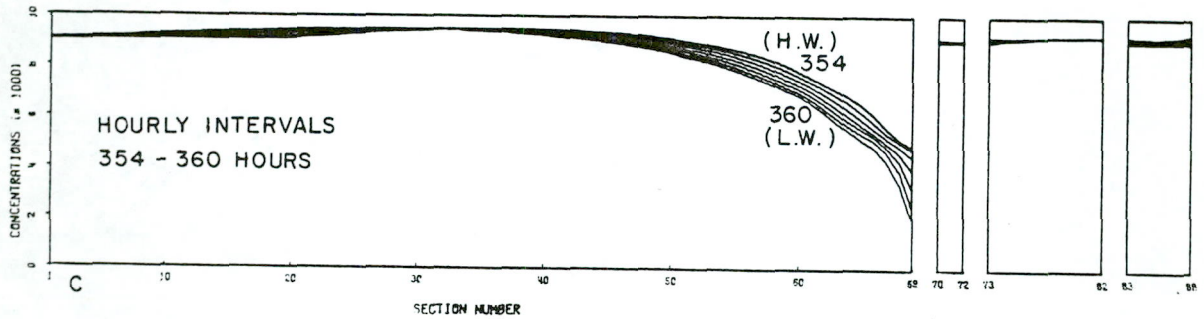

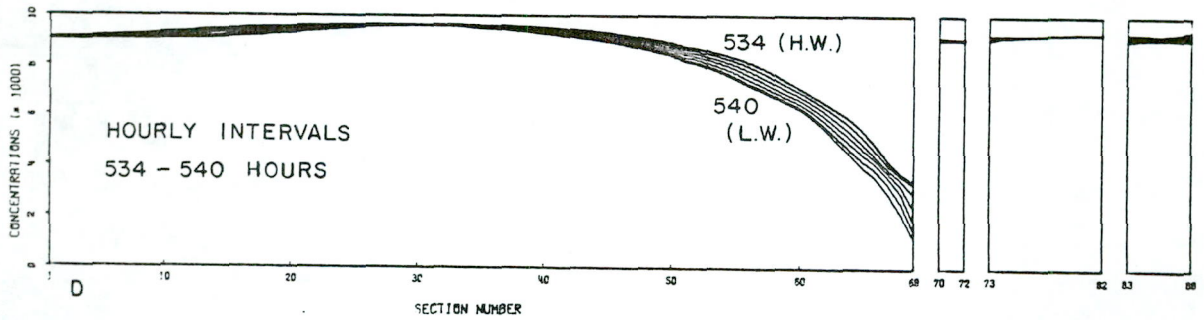

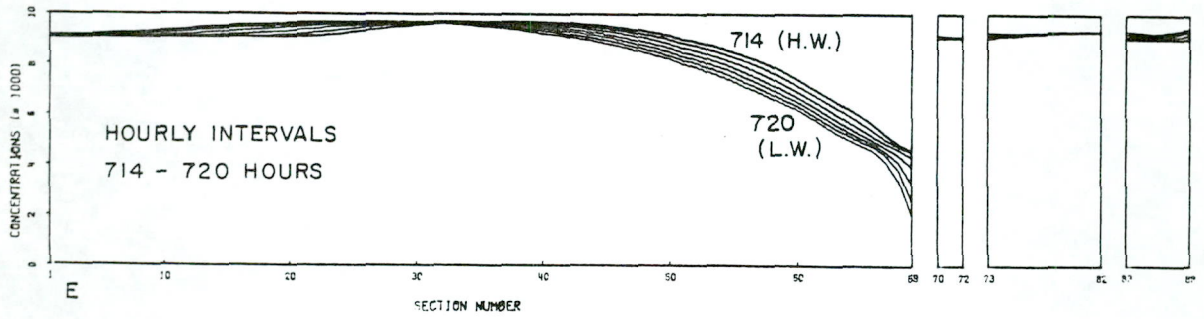

TRACED: JBT CHECKED: DATE: REF:	1-DIMENSIONAL WATER-QUALITY MODEL SWARTKOPS MODEL INFLUENCE OF CONSTANT EVAPORATION RATE (0.156 m / MONTH) ON CONCENTRATIONS RIVER FLOW 0.05 m^3/s DW=6.0 m^2/s	FIGURE 9

NATIONAL RESEARCH INSTITUTE FOR OCEANOLOGY

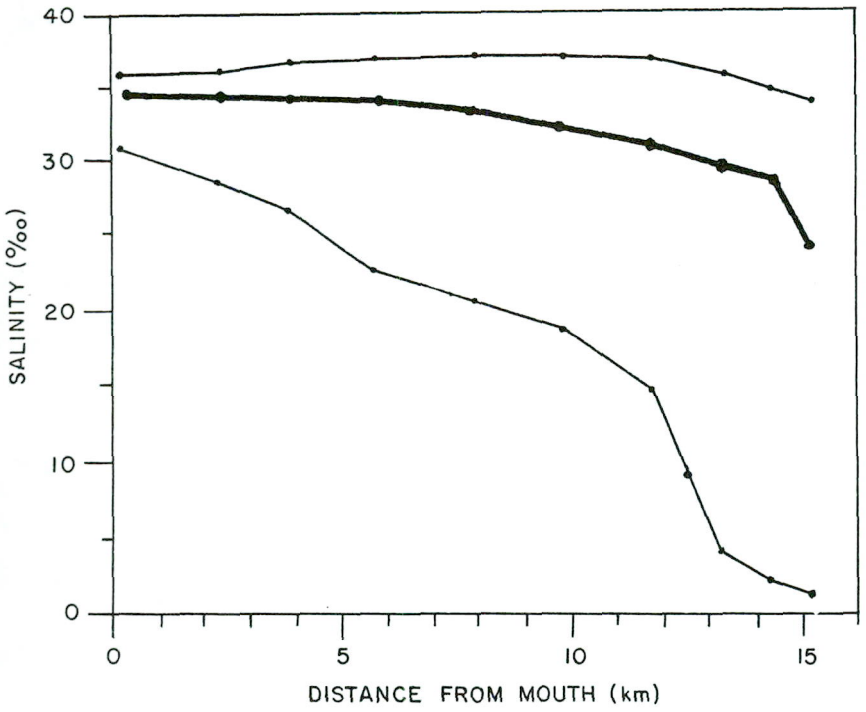

The mean annual salinities (dark line) and salinity ranges (fine line) at 10 stations along the Swartkops estuary from Dec. 1971 to Nov. 1972.

TRACED JBT CHECKED DATE REF	1-DIMENSIONAL WATER-QUALITY MODEL MEASURED SALINITIES IN SWARTKOPS ESTUARY (Mc LACHLAN, 1972)	FIGURE 10

NATIONAL RESEARCH INSTITUTE FOR OCEANOLOGY

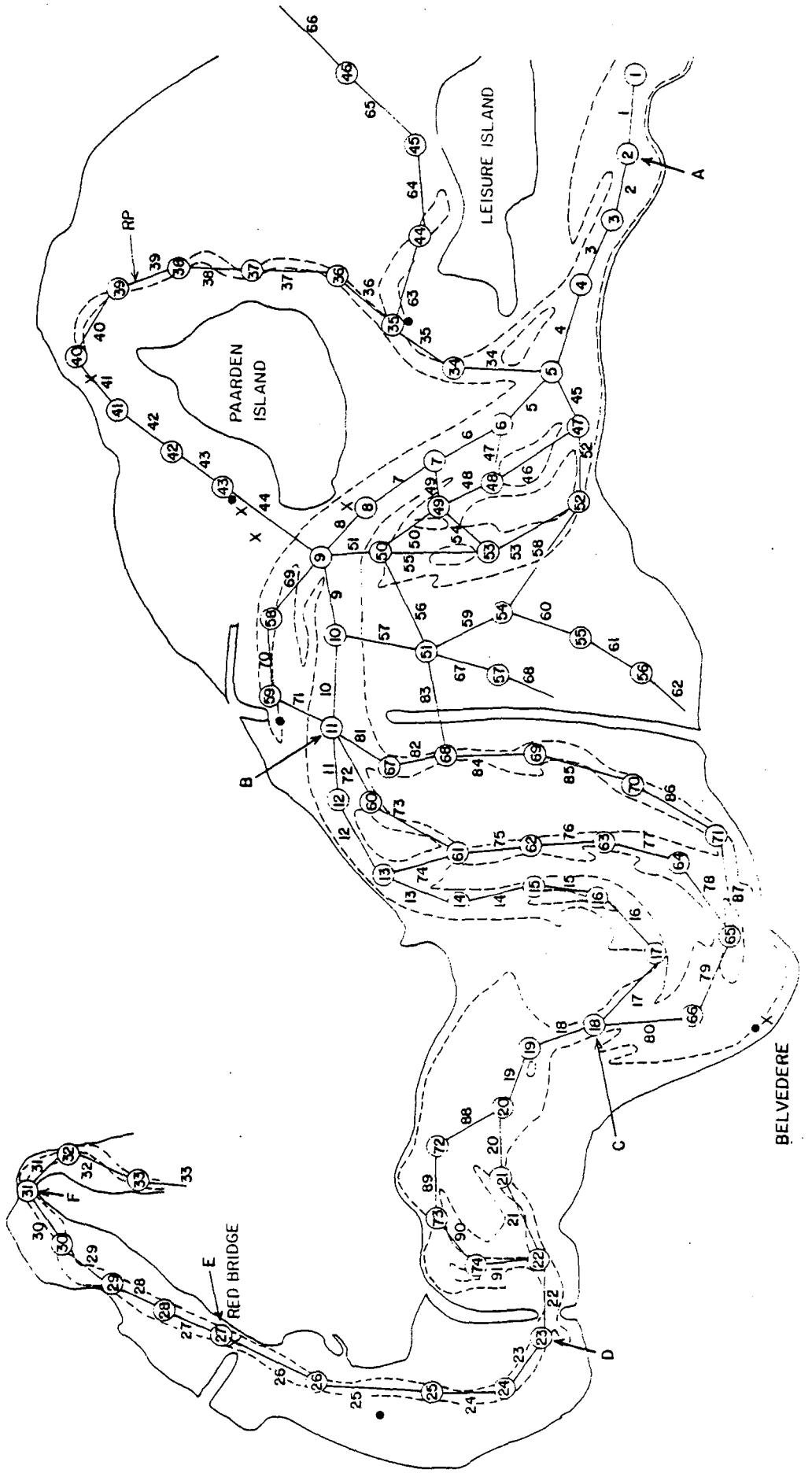

TRACED: JBT CHECKED: DATE: REF:	KNYSNA MODEL SCHEMATIZATION OF THE KNYSNA ESTUARY	FIGURE 11

NATIONAL RESEARCH INSTITUTE FOR OCEANOLOGY

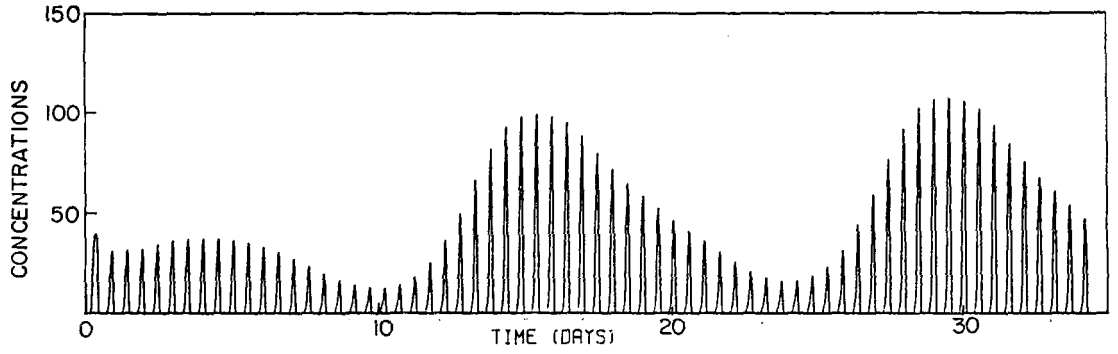

A. POSITION I (HEADS)

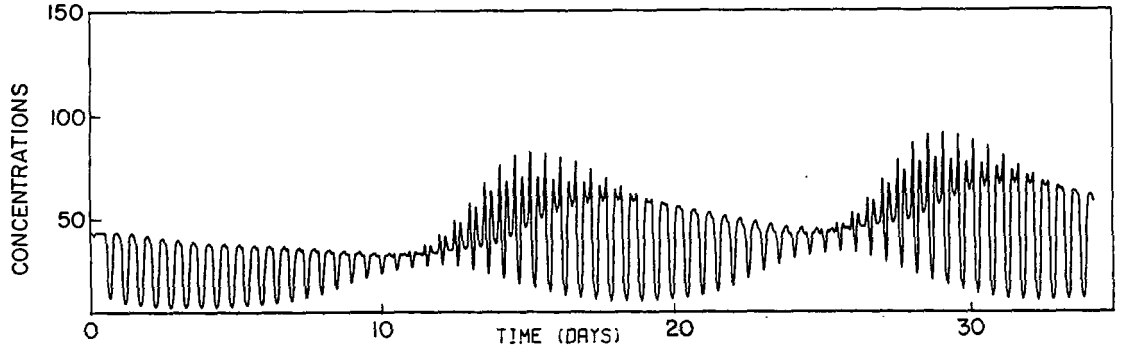

B. POSITION II

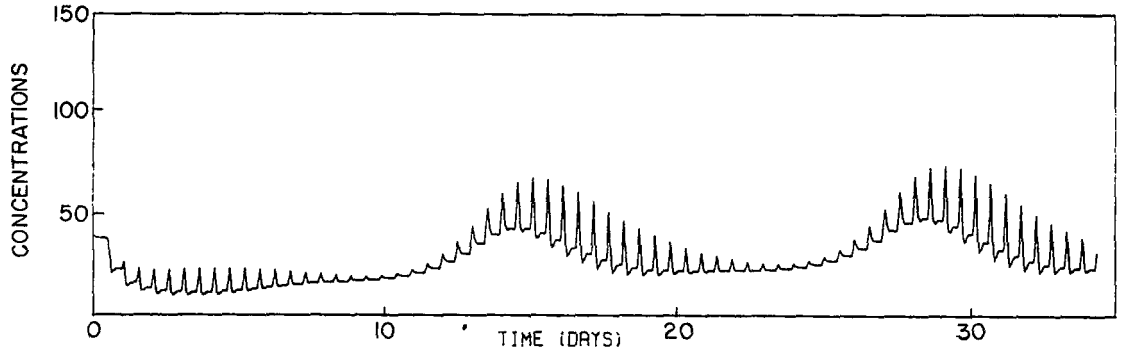

C. POSITION 54

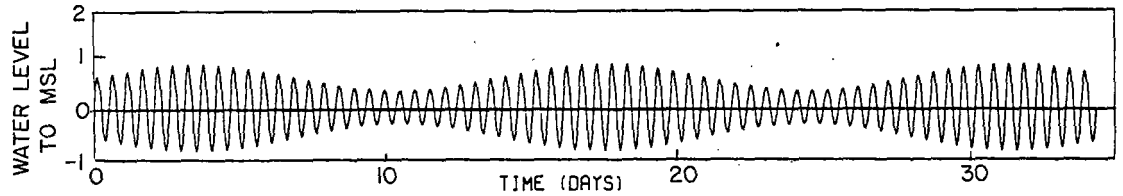

D. WATERLEVEL VARIATION AT HEADS (POSITION I)

TRACED: JBT CHECKED: DATE: REF:	1-DIMENSIONAL WATER-QUALITY MODEL KNYSNA MODEL (FIG. 11) VARIATION OF CONCENTRATIONS WITH TIME AT INDICATED POSITIONS DW = 2.0 m^2/s	FIGURE 12

NATIONAL RESEARCH INSTITUTE FOR OCEANOLOGY

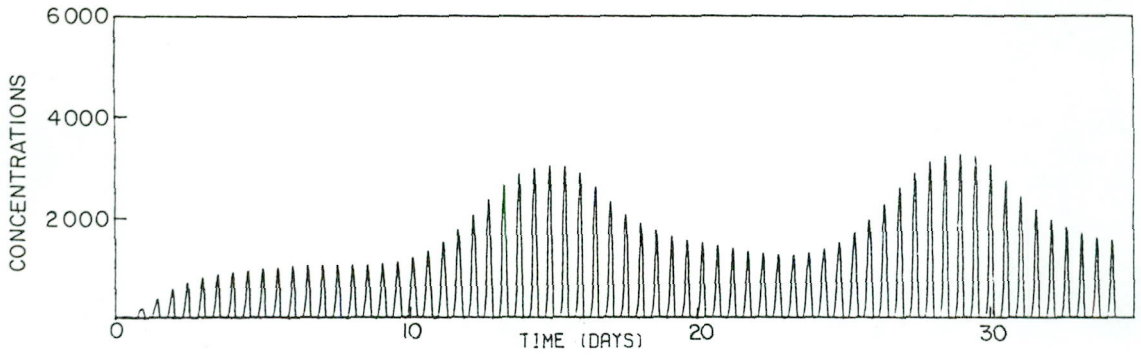

A. POSITION 35

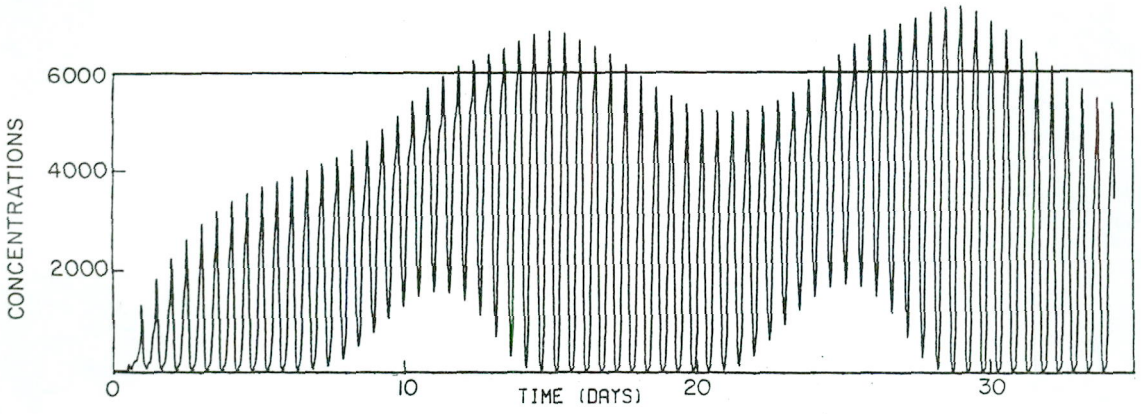

B. POSITION 39

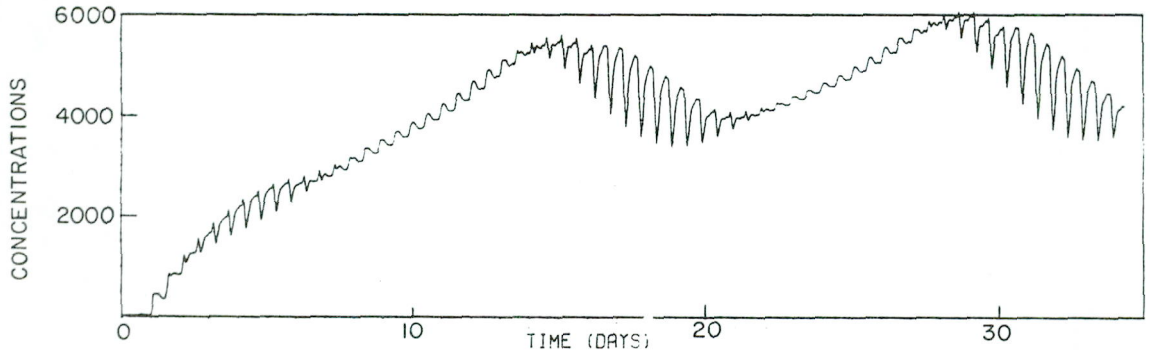

C. POSITION 43

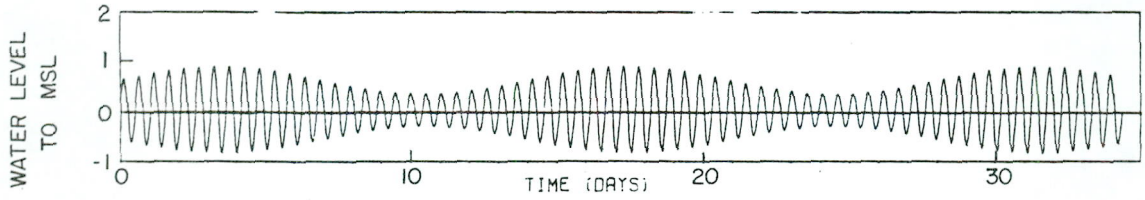

D. WATERLEVEL VARIATION AT HEADS (POSITION 1)

TRACED: JBT CHECKED: DATE: REF:	1-DIMENSIONAL WATER-QUALITY MODEL KNYSNA MODEL (FIG. 11) VARIATION OF CONCENTRATIONS WITH TIME AT INDICATED POSITIONS DW = 2.0	FIGURE 13

NATIONAL RESEARCH INSTITUTE FOR OCEANOLOGY

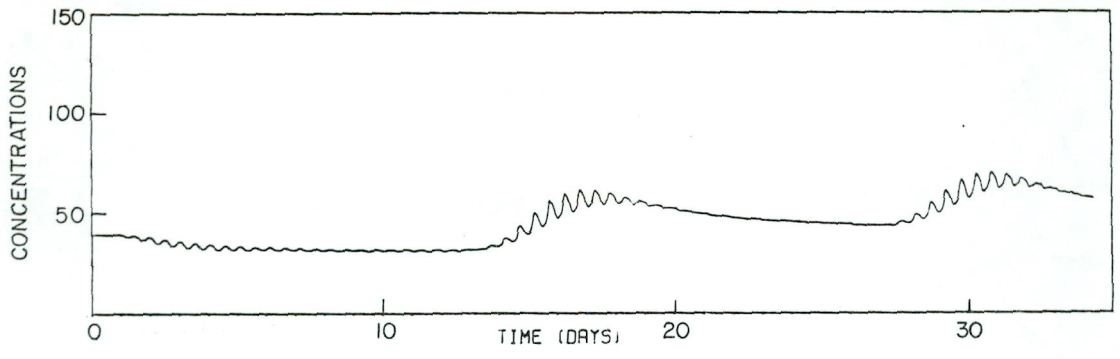

A. POSITION 66

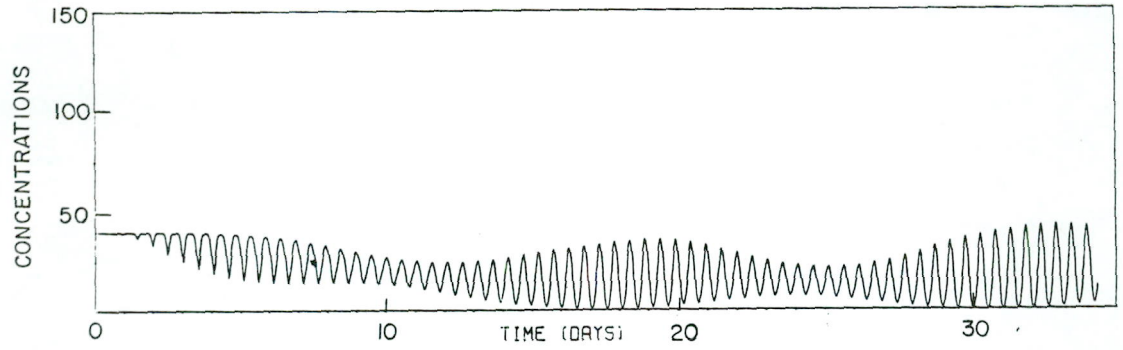

B. POSITION 25

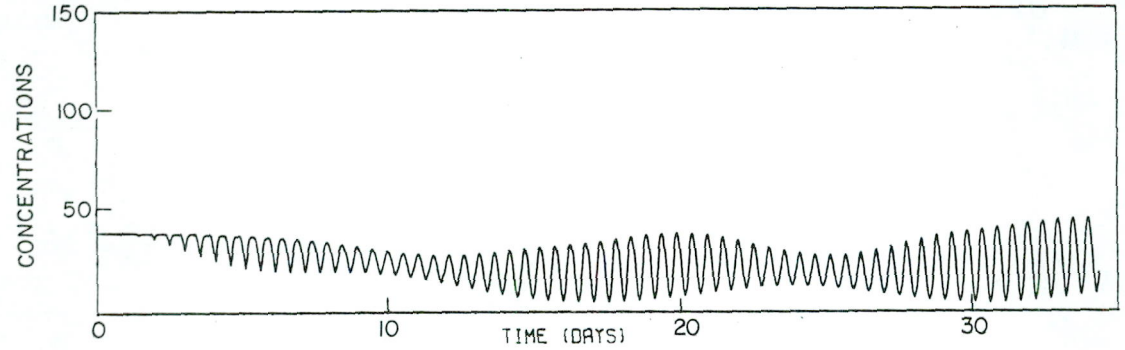

C. POSITION 26

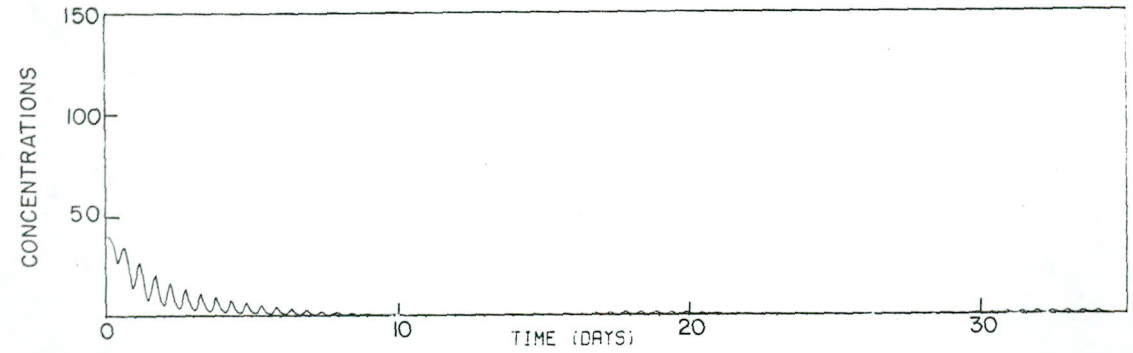

D. POSITION 32

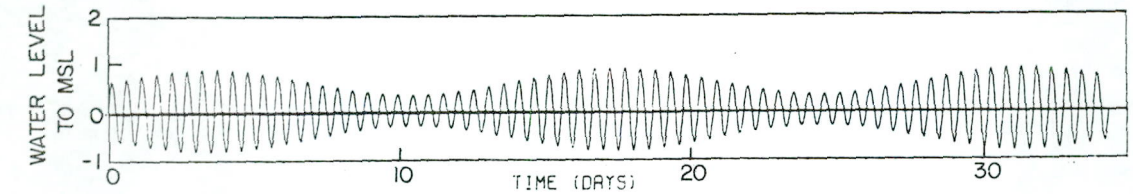

E. WATERLEVEL VARIATION AT HEADS (POSITION 1)

TRACED: JBT CHECKED: DATE: REF:	1-DIMENSIONAL WATER-QUALITY MODEL KNYSNA MODEL (FIG. 11) VARIATION OF CONCENTRATIONS WITH TIME AT INDICATED POSITIONS DW = 2.0	FIGURE 14

NATIONAL RESEARCH INSTITUTE FOR OCEANOLOGY

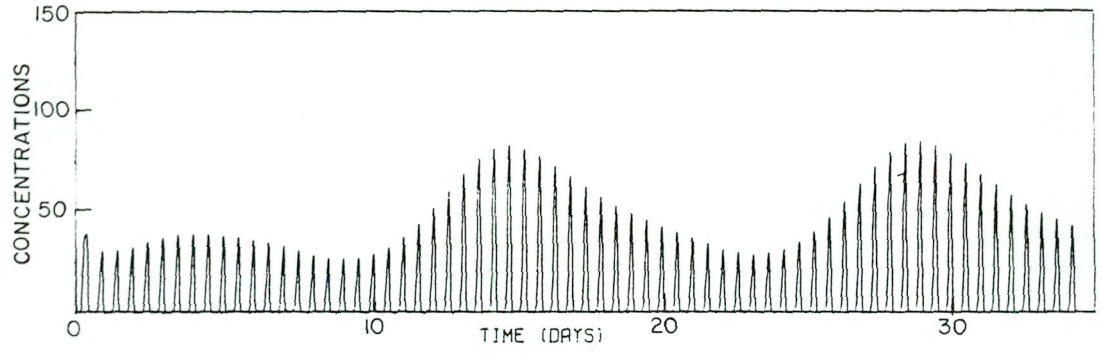

A. POSITION I (HEADS)

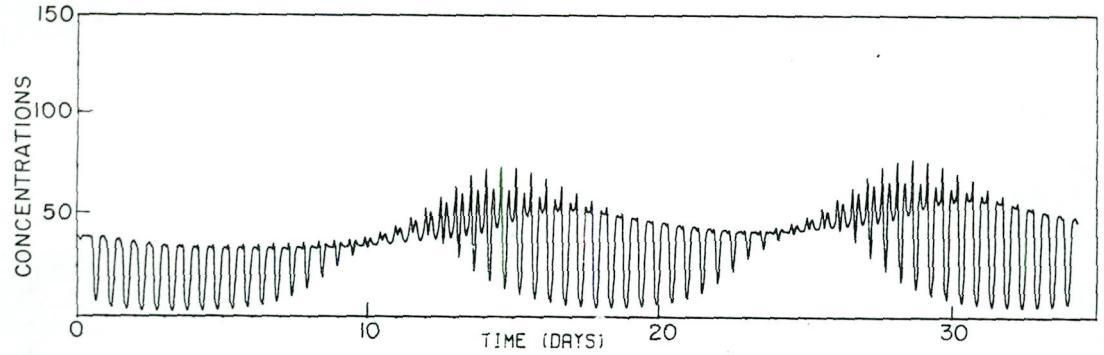

B. POSITION II

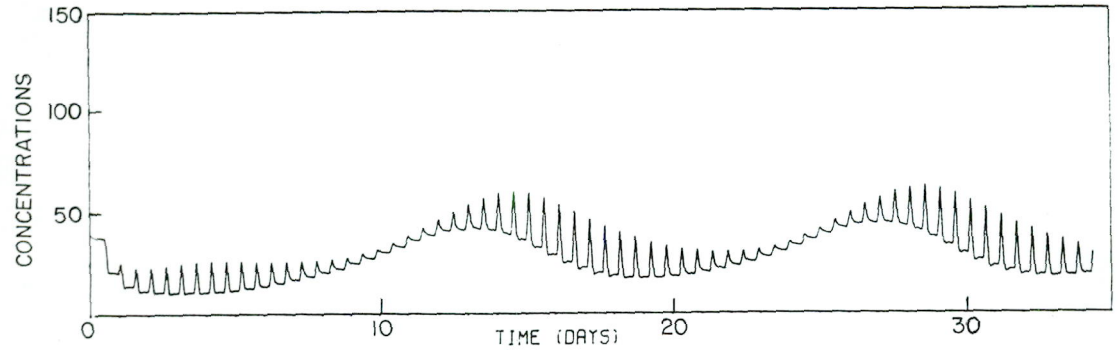

C. POSITION 54

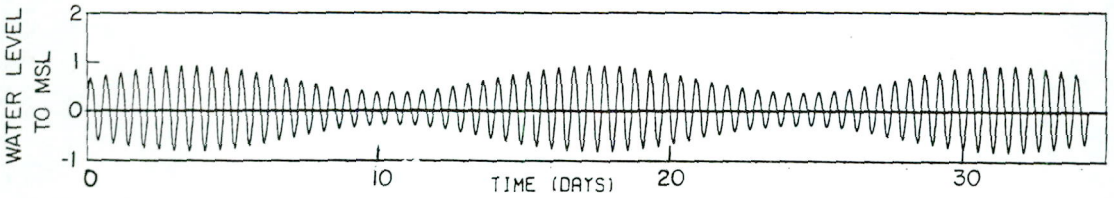

D. WATERLEVEL VARIATION AT HEADS (POSITION I)

TRACED: JBT CHECKED: DATE: REF	1-DIMENSIONAL WATER-QUALITY MODEL KNYSNA MODEL (FIG. 11) VARIATION OF CONCENTRATIONS WITH TIME AT INDICATED POSITIONS DW = 6.0	FIGURE 15

NATIONAL RESEARCH INSTITUTE FOR OCEANOLOGY

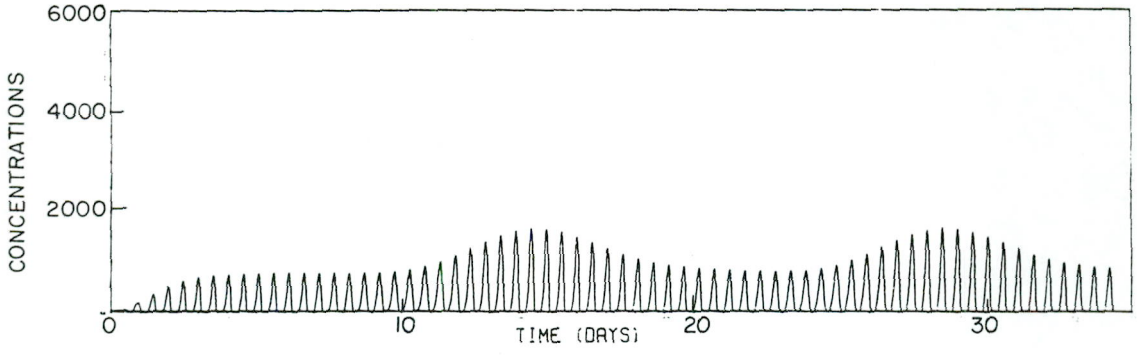

A. POSITION 35

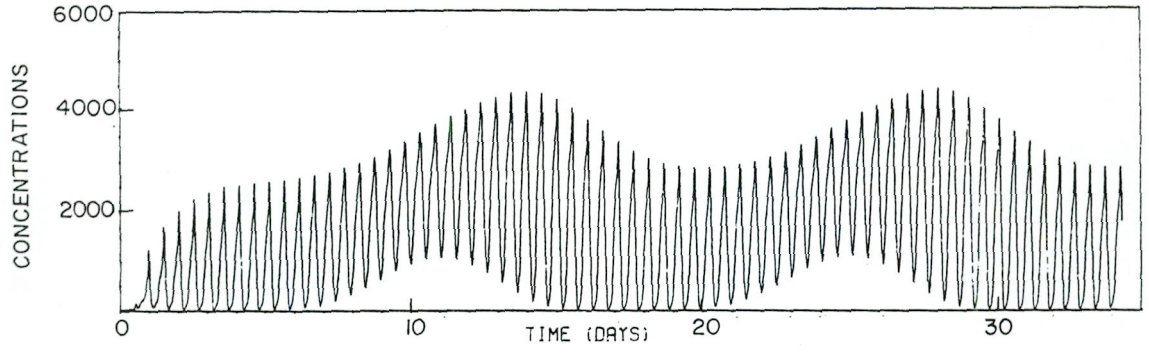

B. POSITION 39

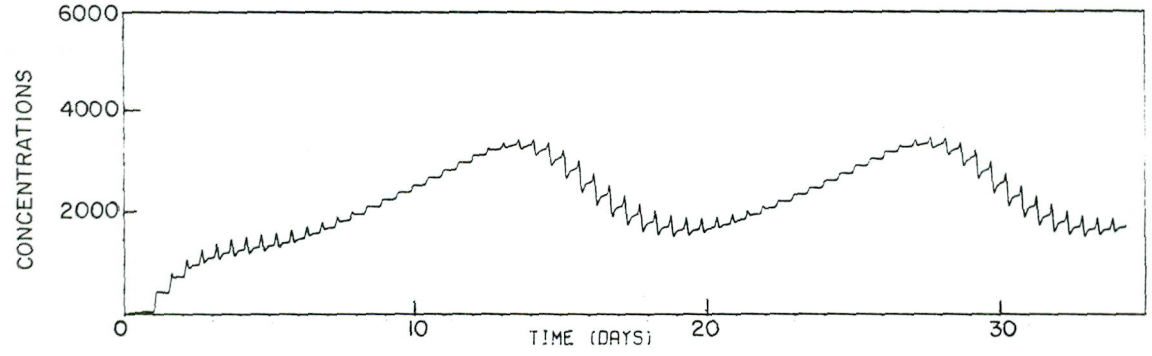

C. POSITION 43

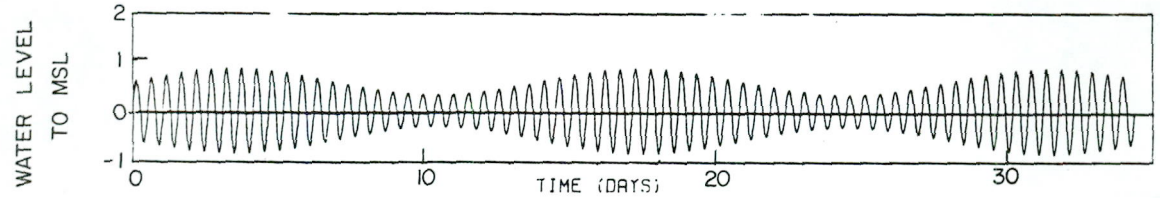

D. WATERLEVEL VARIATION AT HEADS (POSITION 1)

TRACED JBT CHECKED DATE REF	1-DIMENSIONAL WATER-QUALITY MODEL KNYSNA MODEL (FIG. 11) VARIATION OF CONCENTRATIONS WITH TIME AT INDICATED POSITIONS DW = 6.0	FIGURE 16
NATIONAL RESEARCH INSTITUTE FOR OCEANOLOGY		

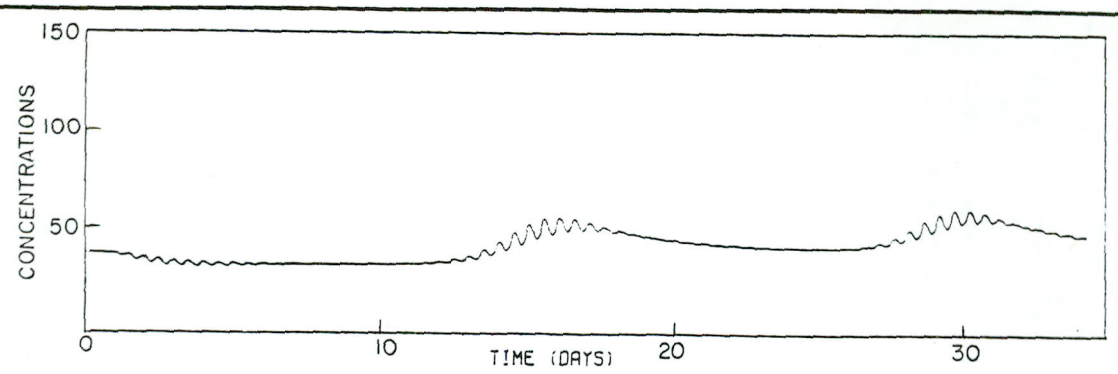

A. POSITION 66 (BELVEDERE)

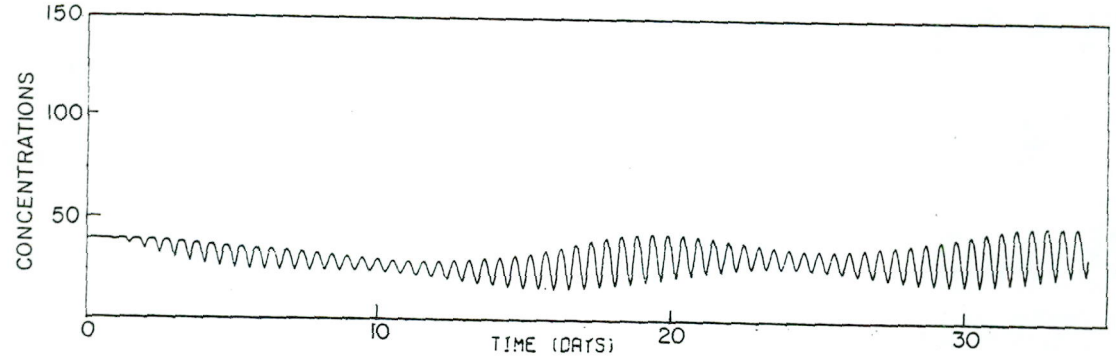

B. POSITION 25

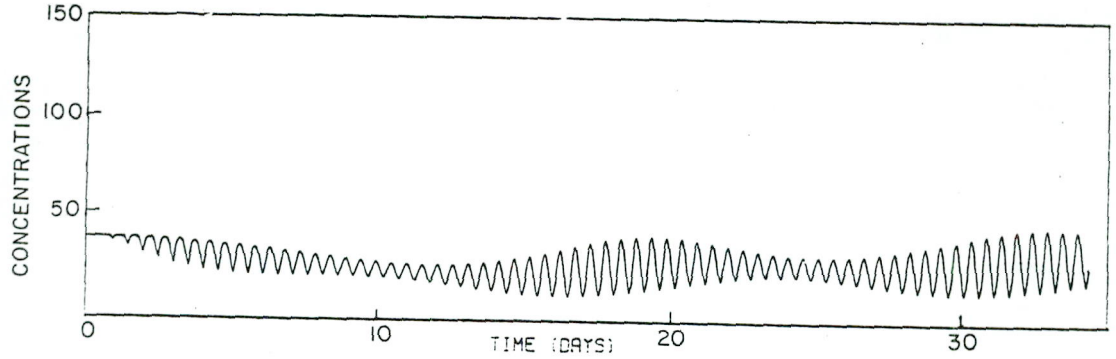

C. POSITION 26

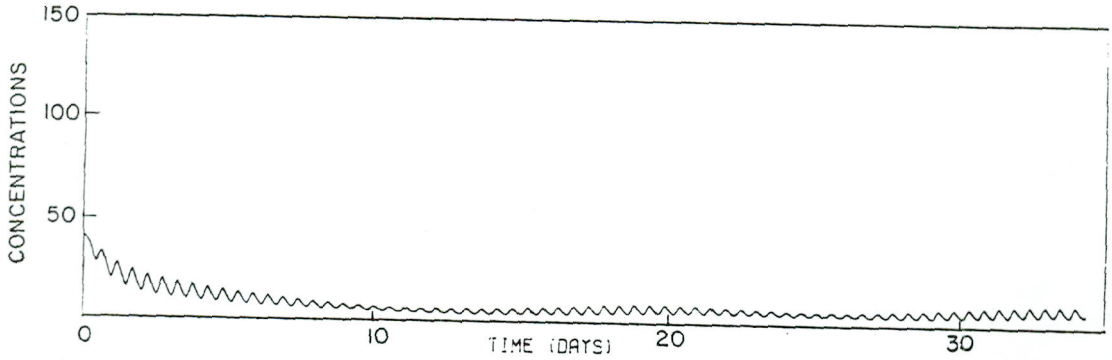

D. POSITION 32

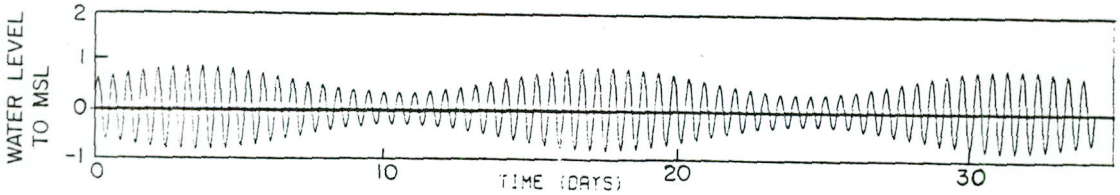

E. WATERLEVEL VARIATION AT HEADS (POSITION 1)

TRACED JBT CHECKED DATE REF	1-DIMENSIONAL WATER-QUALITY MODEL KNYSNA MODEL (FIG. 11) VARIATION OF CONCENTRATIONS WITH TIME AT INDICATED POSITIONS DW = 6.0	FIGURE 17

NATIONAL RESEARCH INSTITUTE FOR OCEANOLOGY

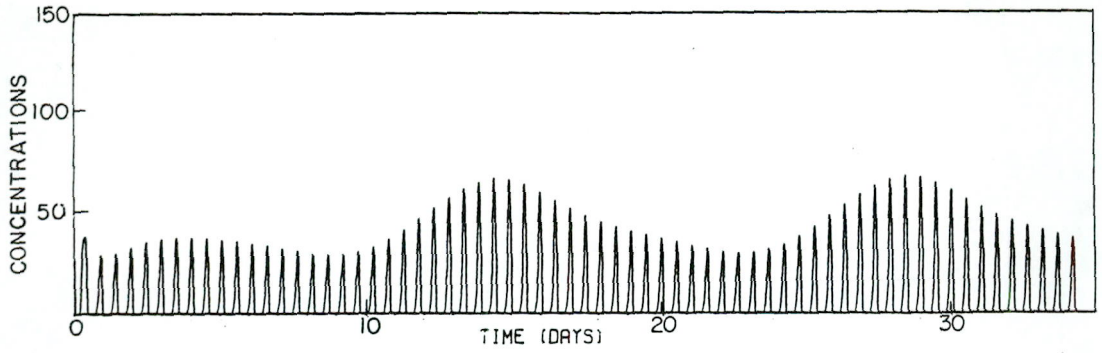

A. POSITION 1 (HEADS)

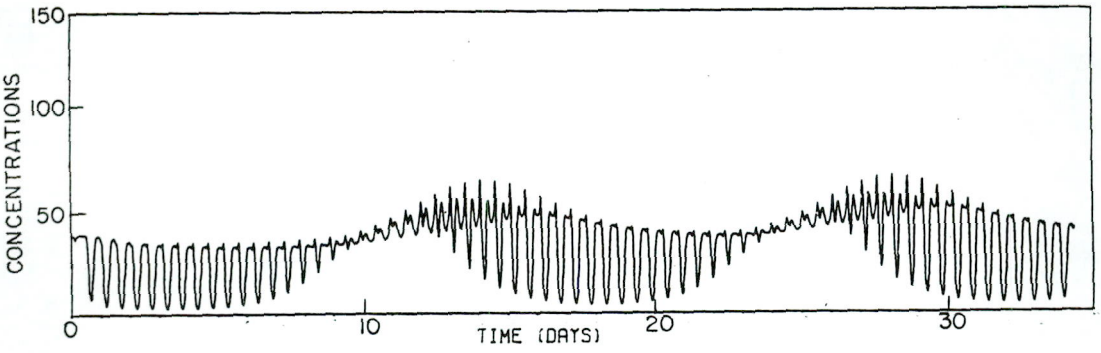

B. POSITION 11

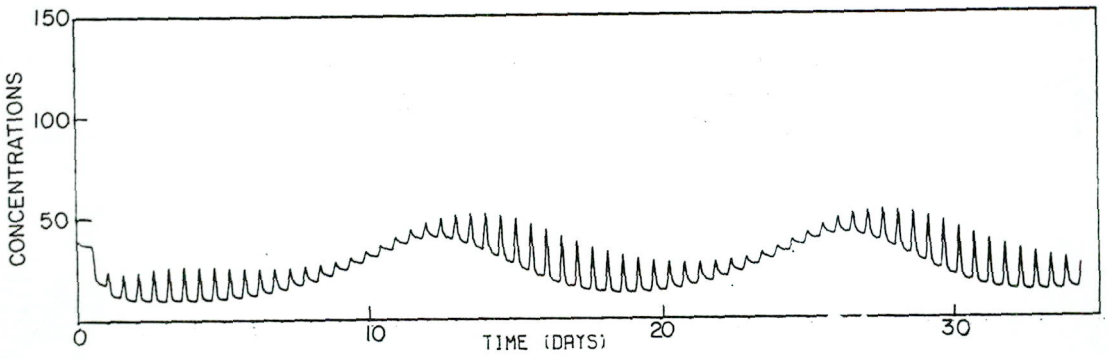

C. POSITION 54

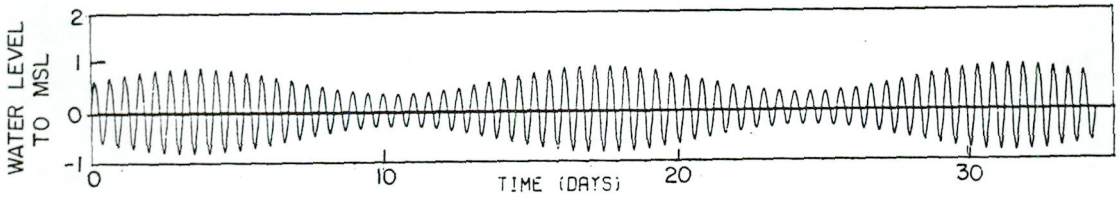

D. WATERLEVEL VARIATION AT HEADS (POSITION 1)

TRACED: JBT CHECKED: DATE: REF:	1-DIMENSIONAL WATER-QUALITY MODEL KNYSNA MODEL (FIG. 11) VARIATION OF CONCENTRATIONS WITH TIME AT INDICATED POSITIONS DW = 12.0	FIGURE 18

NATIONAL RESEARCH INSTITUTE FOR OCEANOLOGY

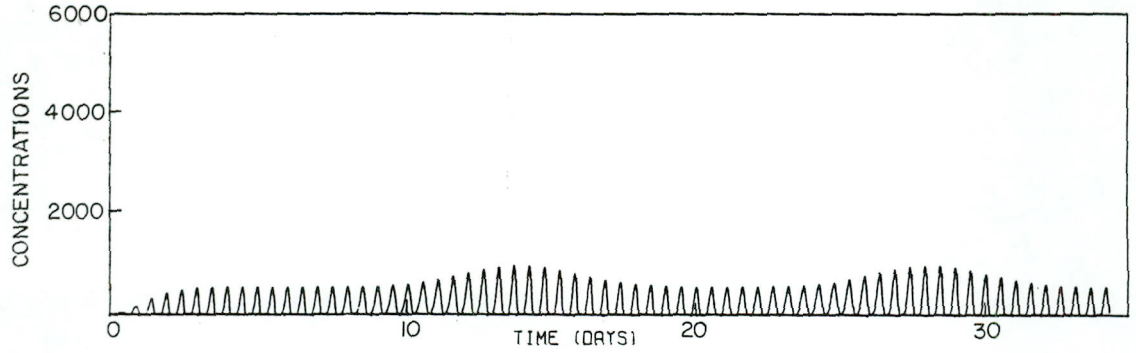

A. POSITION 35

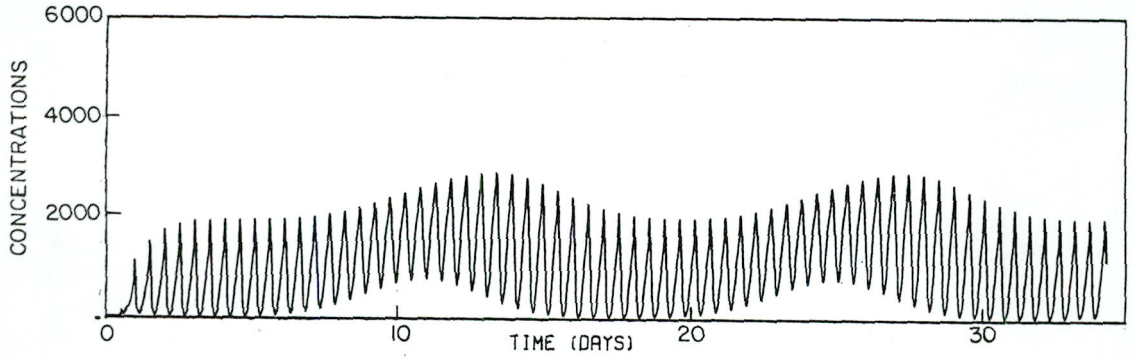

B. POSITION 39

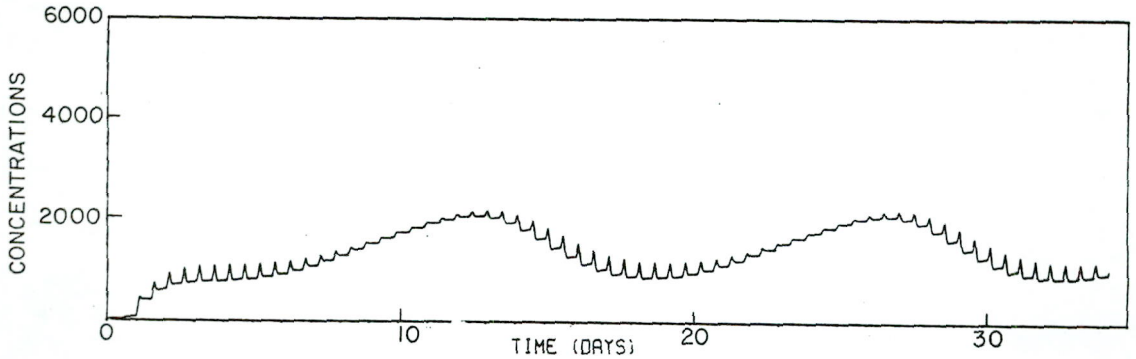

C. POSITION 43

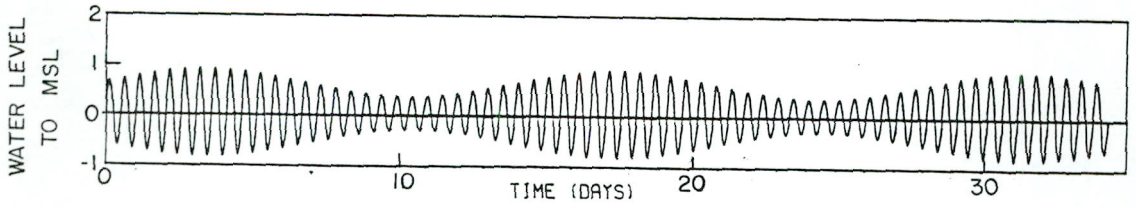

D. WATERLEVEL VARIATION AT HEADS (POSITION 1)

TRACED JBT CHECKED DATE REF	1-DIMENSIONAL WATER-QUALITY MODEL KNYSNA MODEL (FIG. 11) VARIATION OF CONCENTRATIONS WITH TIME AT INDICATED POSITIONS DW=12.0	FIGURE 19

NATIONAL RESEARCH INSTITUTE FOR OCEANOLOGY

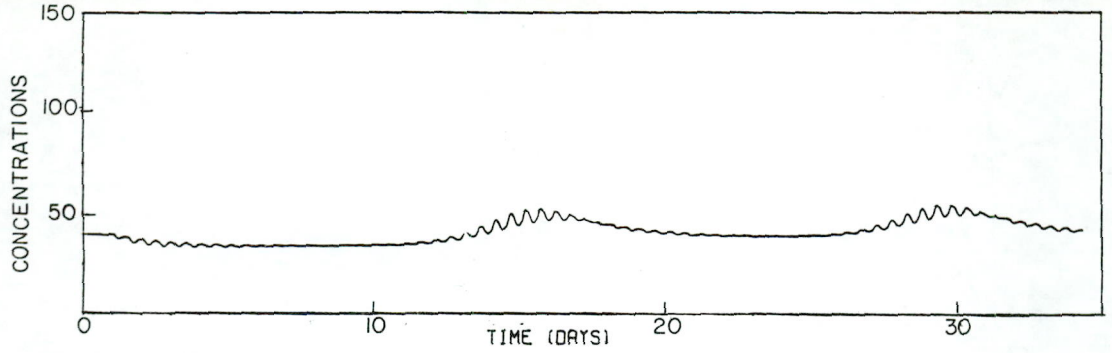

A. POSITION 66 (BELVEDERE)

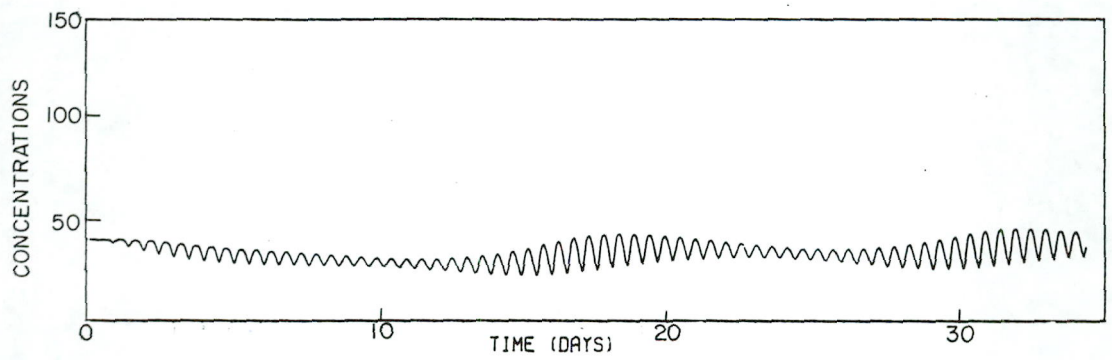

B. POSITION 25

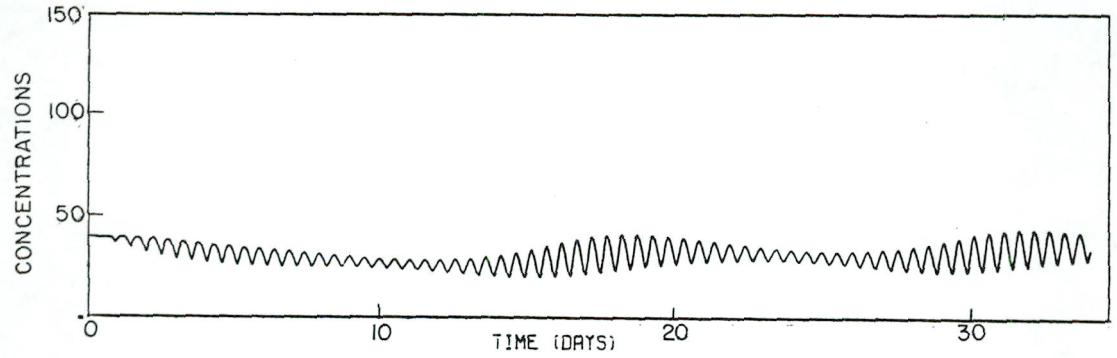

C. POSITION 26

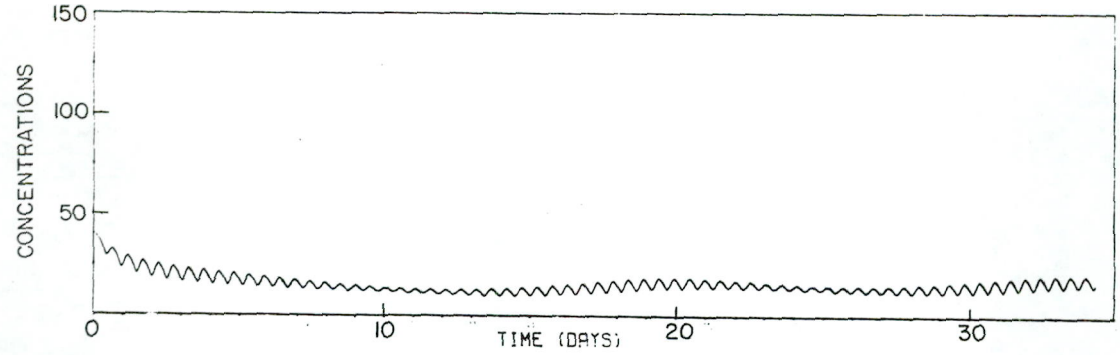

D. POSITION 32

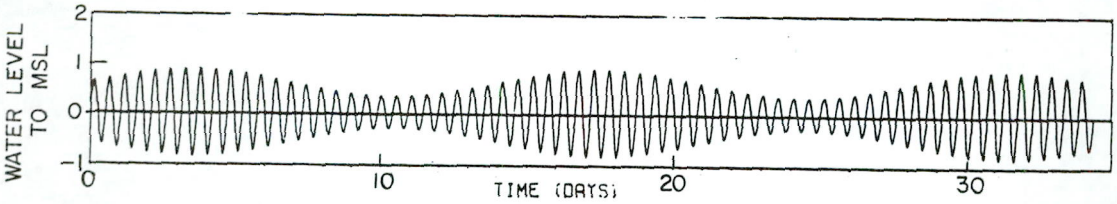

E. WATERLEVEL VARIATION AT HEADS (POSITION 1)

TRACED. JBT CHECKED DATE REF	1 - DIMENSIONAL WATER - QUALITY MODEL KNYSNA MODEL (FIG. 11) VARIATION OF CONCENTRATIONS WITH TIME AT INDICATED POSITIONS DW = 12.0	FIGURE 20

NATIONAL RESEARCH INSTITUTE FOR OCEANOLOGY

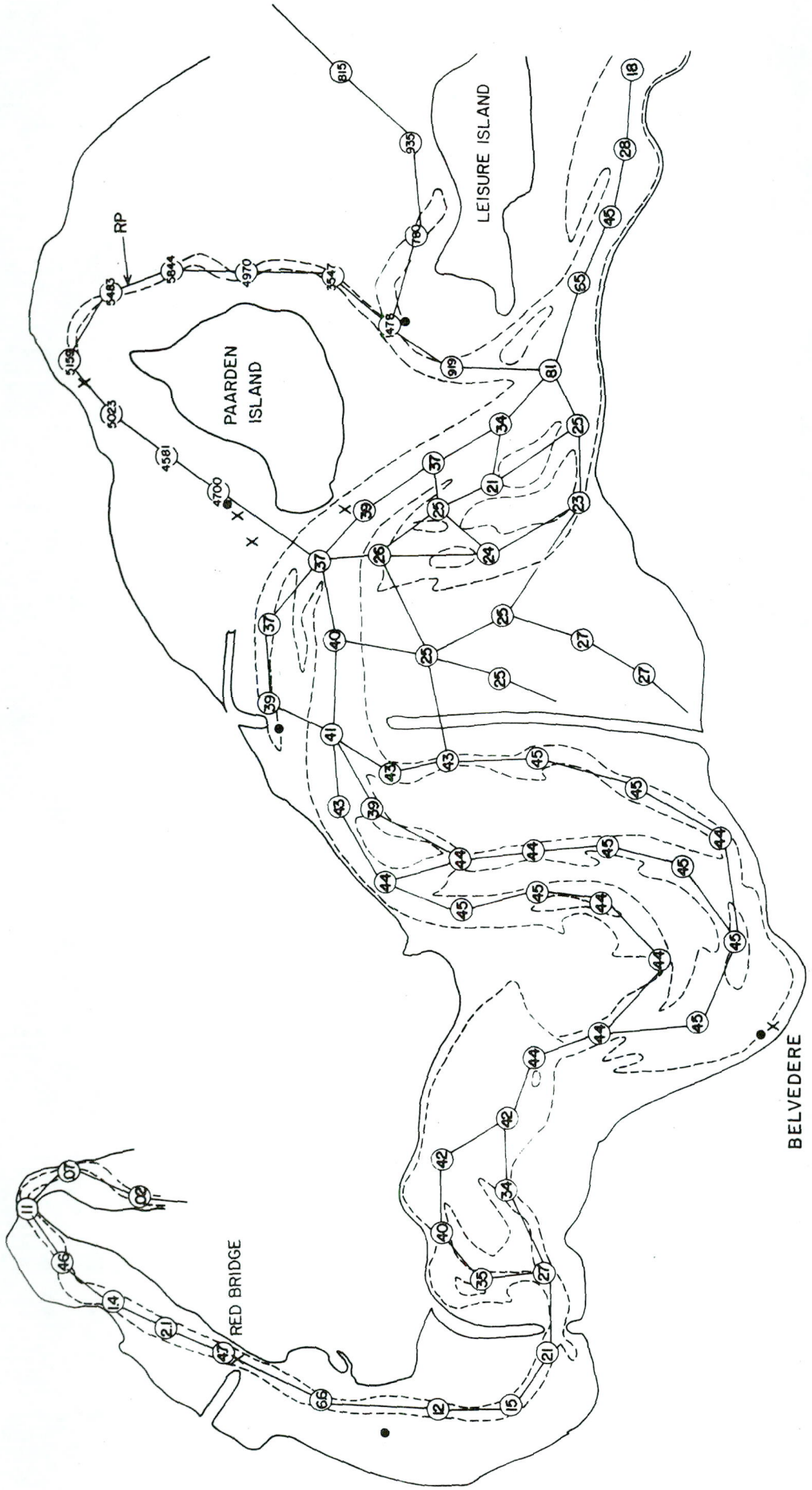

TRACED: JBT CHECKED: DATE: REF:	1-DIMENSIONAL WATER-QUALITY MODEL KNYSNA MODEL DISTRIBUTION OF CONCENTRATIONS AT LOW WATER NEAPTIDE (AT 597 HOURS) DW = 2.0	FIGURE 21

NATIONAL RESEARCH INSTITUTE FOR OCEANOLOGY

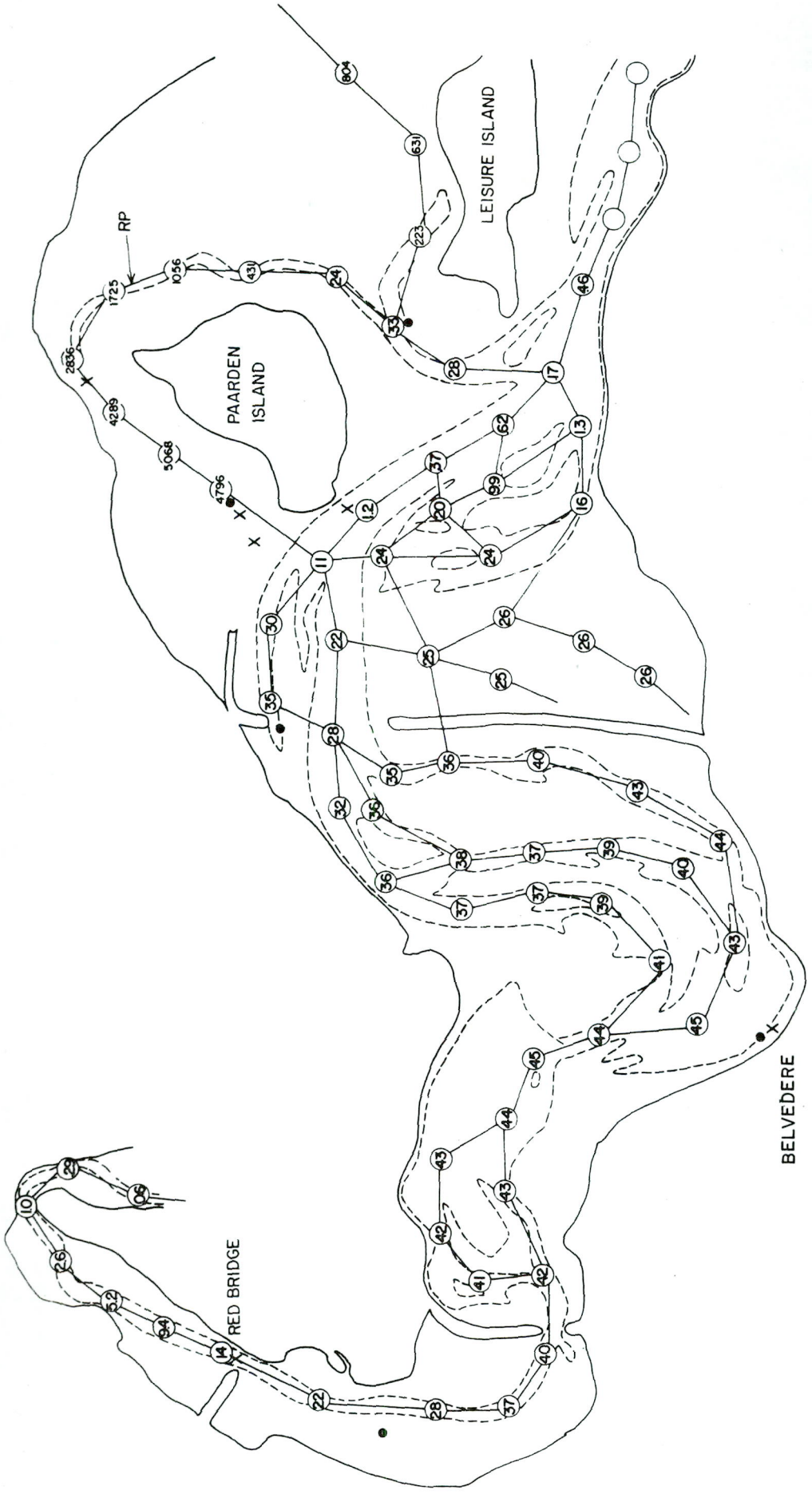

TRACED: JBT CHECKED: DATE: REF:	1-DIMENSIONAL WATER-QUALITY MODEL KNYSNA MODEL DISTRIBUTION OF CONCENTRATIONS AT HIGH WATER NEAPTIDE (AT 591 HOURS) DW = 2.0	FIGURE 22

NATIONAL RESEARCH INSTITUTE FOR OCEANOLOGY

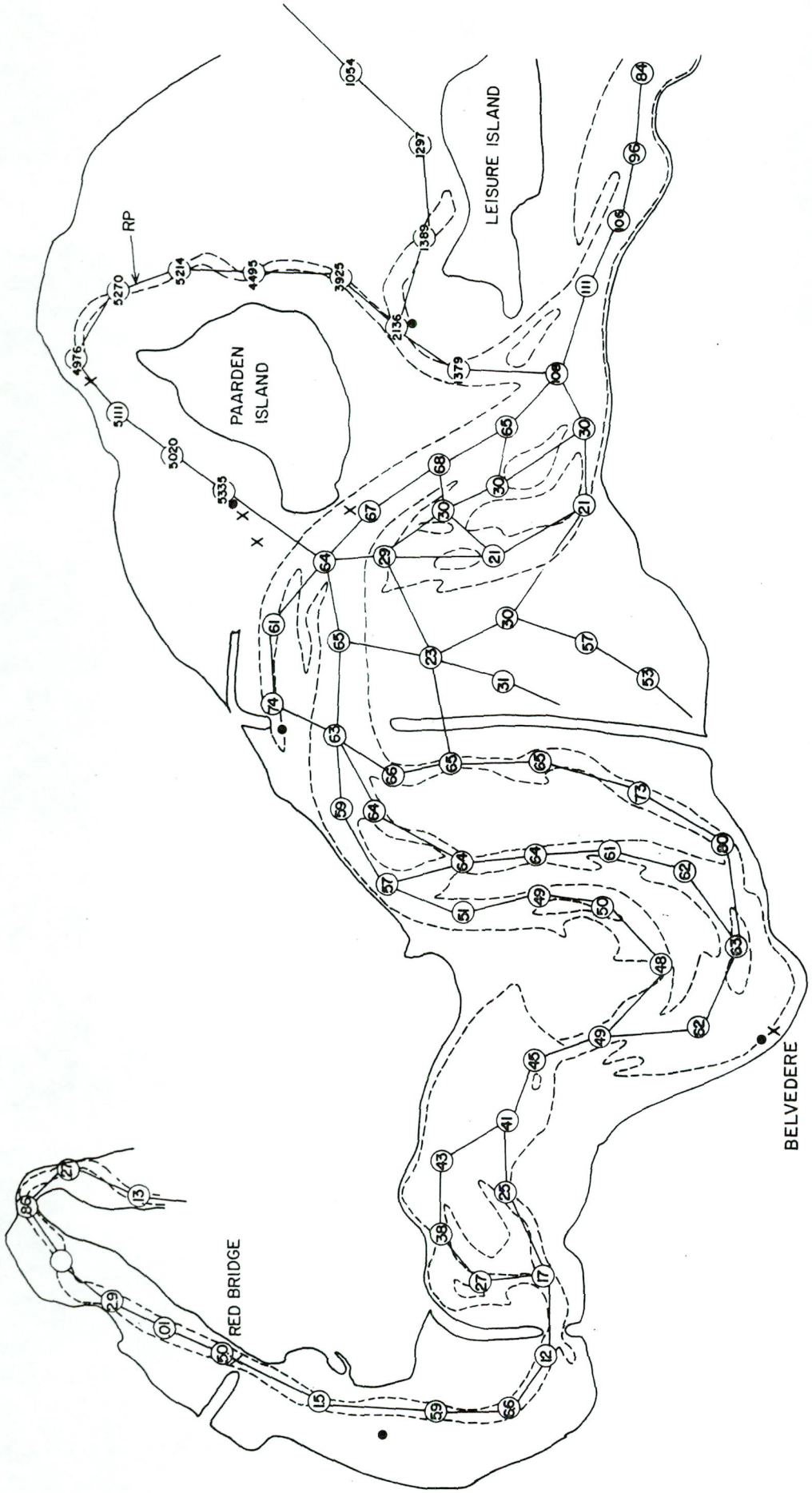

TRACED: JBT
CHECKED:
DATE:
REF:

1-DIMENSIONAL WATER-QUALITY MODEL

KNYSNA MODEL DISTRIBUTION OF CONCENTRATIONS AT LOW WATER SPRINGTIDE (AT 760 HOURS)

DW = 2.0

FIGURE 23

NATIONAL RESEARCH INSTITUTE FOR OCEANOLOGY

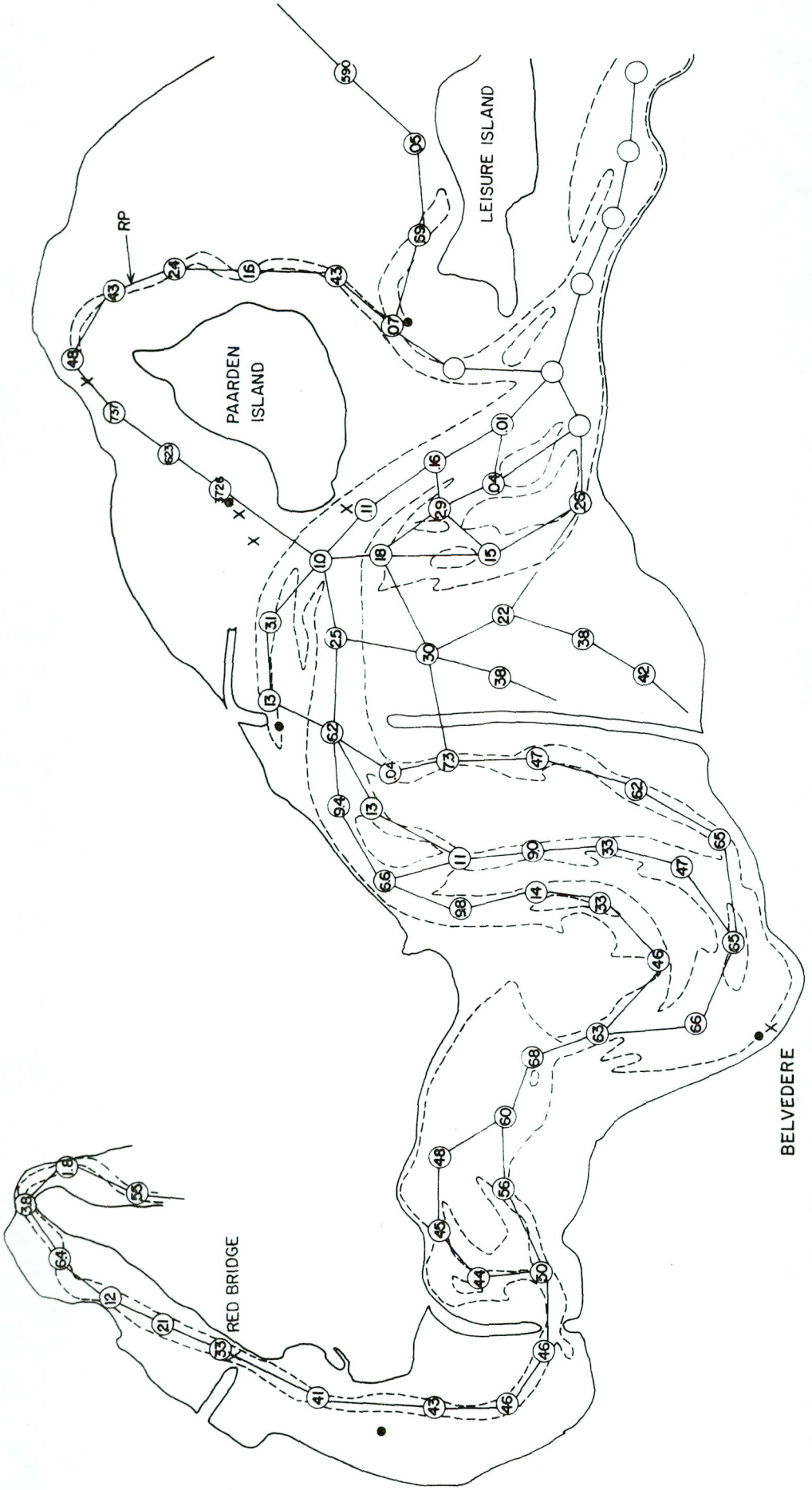

TRACED: JBT CHECKED: DATE: REF:	1-DIMENSIONAL WATER-QUALITY MODEL KNYSNA MODEL DISTRIBUTION OF CONCENTRATIONS AT HIGH WATER SPRINGTIDE (AT 766 HOURS) DW = 2.0	FIGURE 24

NATIONAL RESEARCH INSTITUTE FOR OCEANOLOGY

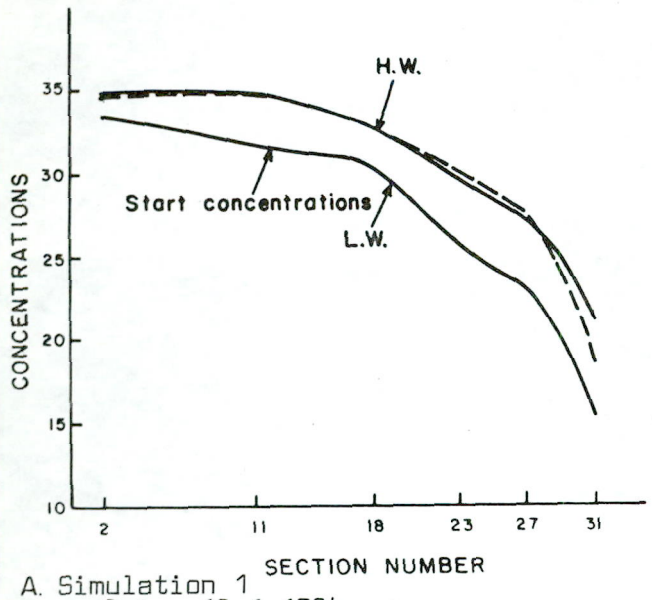

A. Simulation 1
Date: 18.1.1984
Start conditions at L.W.
K = 45.00 for all sections
Flow = 0.8 m^3/s.

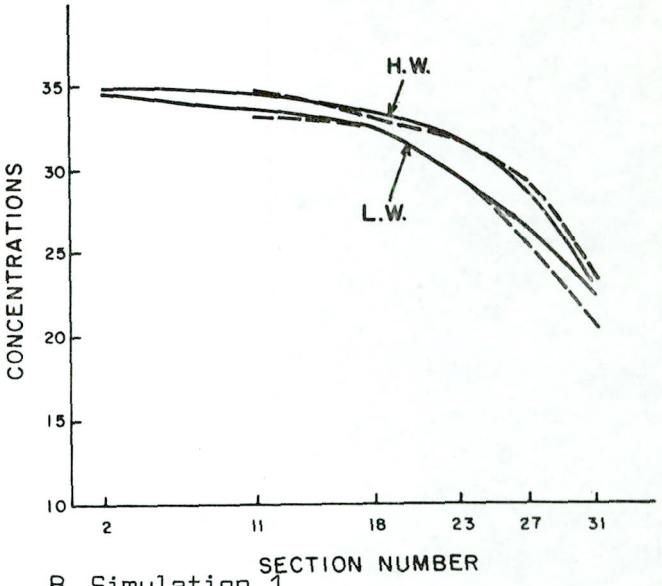

B. Simulation 1
Date: 25.1.1984
K = 45.00 for all sections
Flow = 0.8 m^3/s.

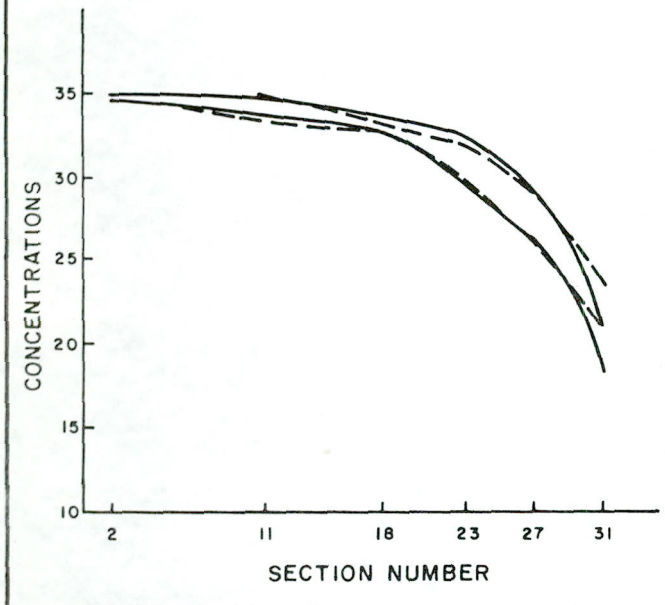

C. Simulation 2
Date: 25.1.1984
K = 45.00 sections 1-22, 33-74
K = 35.00 Sections 23-26
K = 25.00 Sections 27-32
Flow = 0.8 m^3/s.

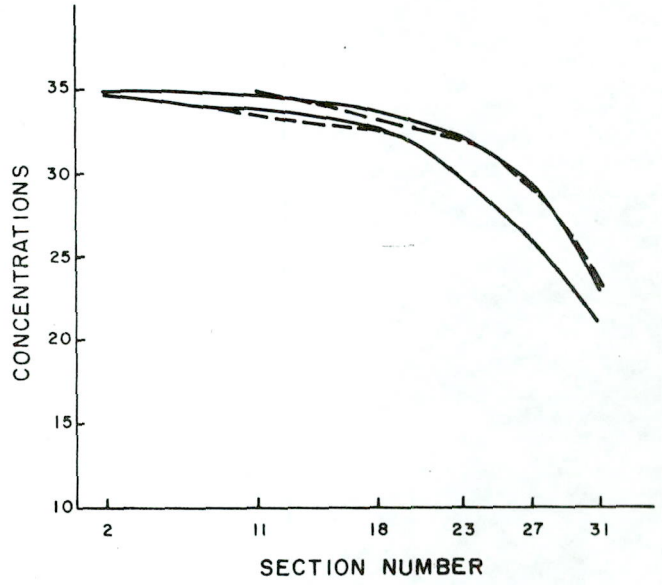

D. Simulation 3
Date: 25.1.1984
K = 45.00 Sections 1-22, 33-74
K = 40.00 Sections 23-26
K = 35.00 Sections 27-32
Flow = 0.8 m^3/s.

——— = computed concentrations
– – – – = field measurements

TRACED H.R.S CHECKED DATE REF	1-DIMENSIONAL WATER-QUALITY MODEL KNYSNA MODEL, LONGITUDINAL SALINITY PROFILES CALIBRATION OF MODEL ON SALINITY DISTRIBUTIONS BY COMPARING MODEL RESULTS WITH FIELD MEASUREMENTS	FIGURE 25

NATIONAL RESEARCH INSTITUTE FOR OCEANOLOGY

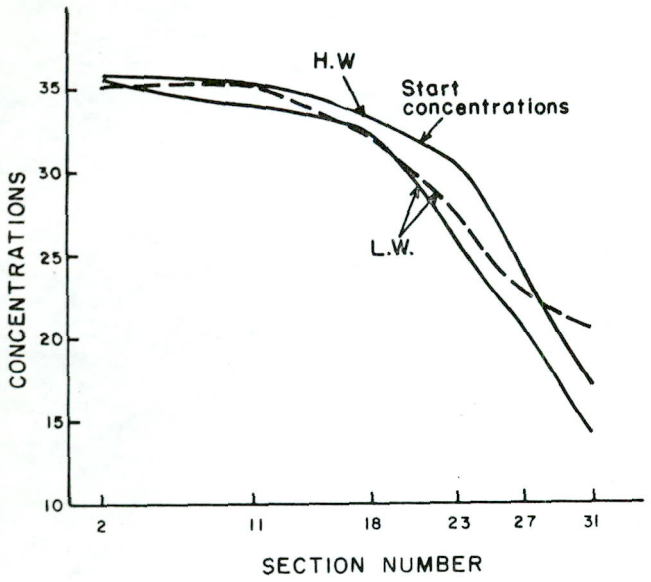

A. Simulation 4
Date: 10.3.1984
Start conditions at H.W.
K = 45.00 Sections 1-22, 33-74
K = 40.00 Sections 23-26
K = 35.00 Sections 27-32

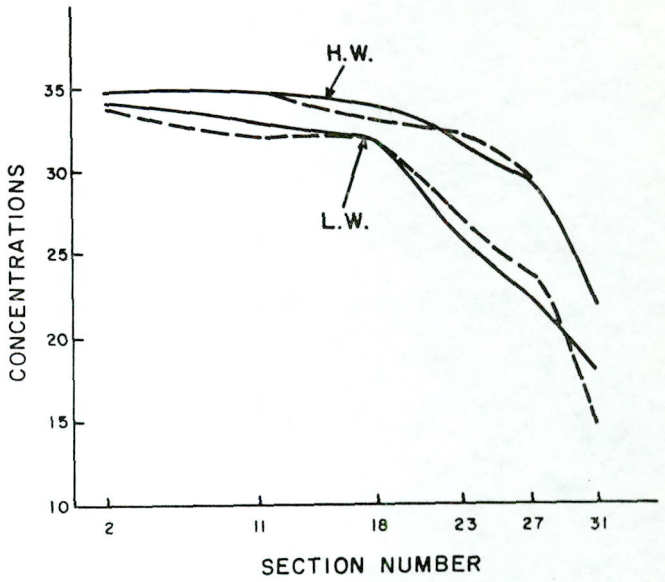

B. Simulation 4
Date: 17.3.1984
Flow: Variable

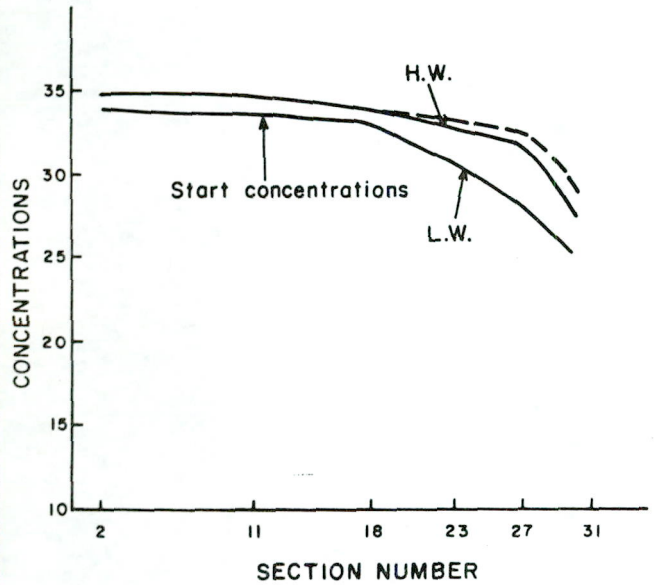

C. Simulation 5
Date: 16.4.1984
K = same as simulation 4
Flow: variable.

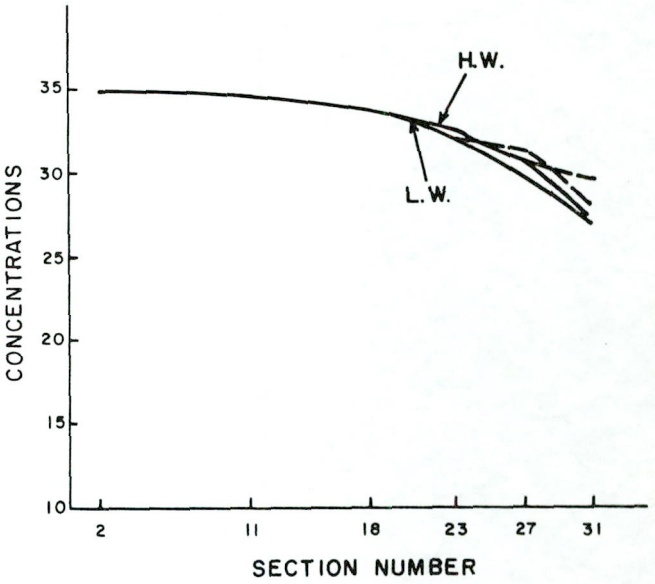

D. Simulation 5
Date: 23.4.1984
K = same as simulation 4
Flow: variable.

——— = computed concentrations
---- = field measurements

TRACED H.R.S CHECKED DATE REF	1-DIMENSIONAL WATER-QUALITY MODEL KNYSNA MODEL, LONGITUDINAL SALINITY PROFILES CALIBRATION OF MODEL ON SALINITY DISTRIBUTIONS BY COMPARING MODEL RESULTS WITH FIELD MEASUREMENTS	FIGURE 26

NATIONAL RESEARCH INSTITUTE FOR OCEANOLOGY

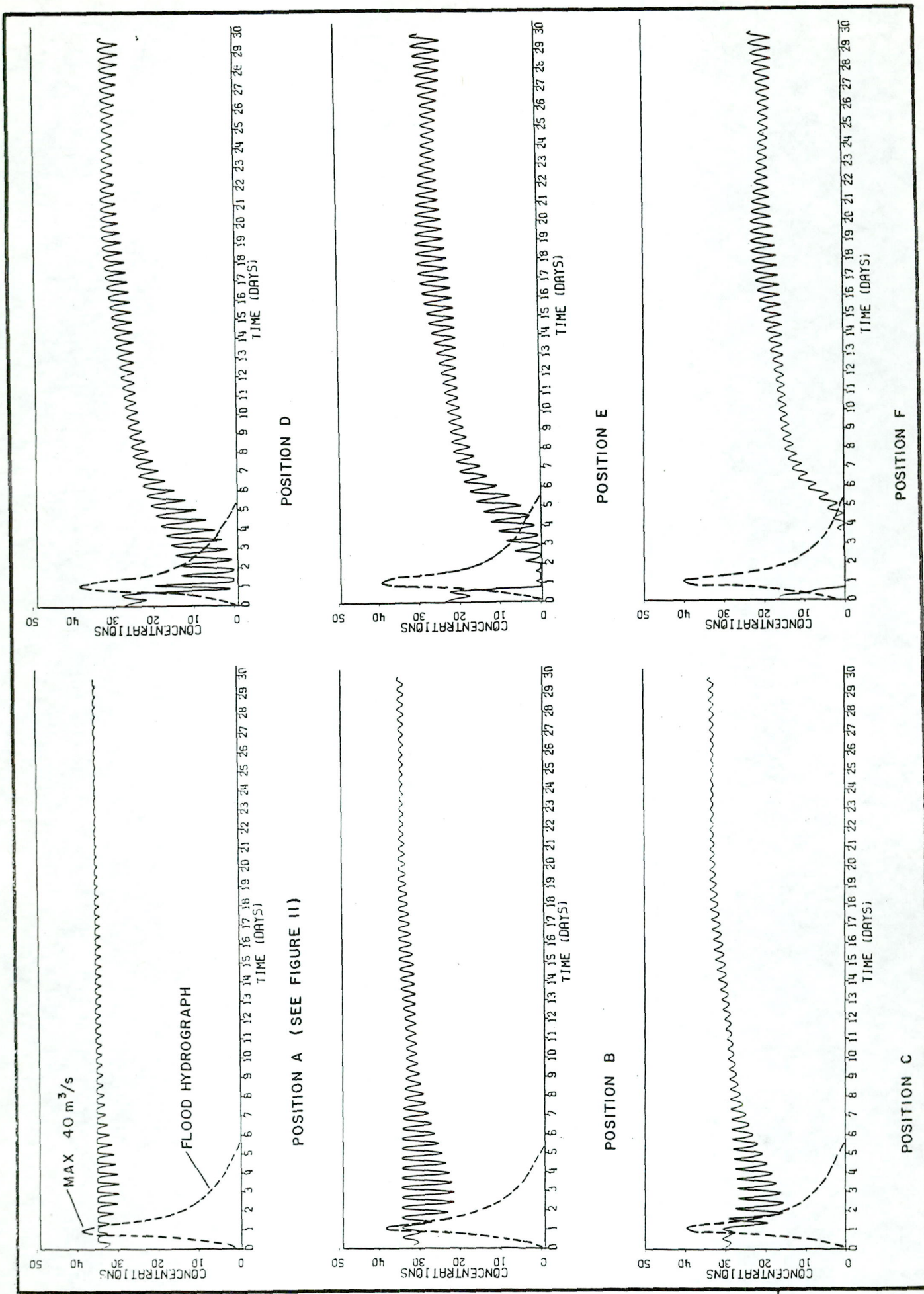

TRACED: JGAM CHECKED: DATE: REF.:	1 - DIMENSIONAL WATER-QUALITY MODEL KNYSNA MODEL INFLUENCE OF A 1:2 YEAR RIVER FLOOD ON SALINITY CONCENTRATIONS	FIGURE 27

NATIONAL RESEARCH INSTITUTE FOR OCEANOLOGY

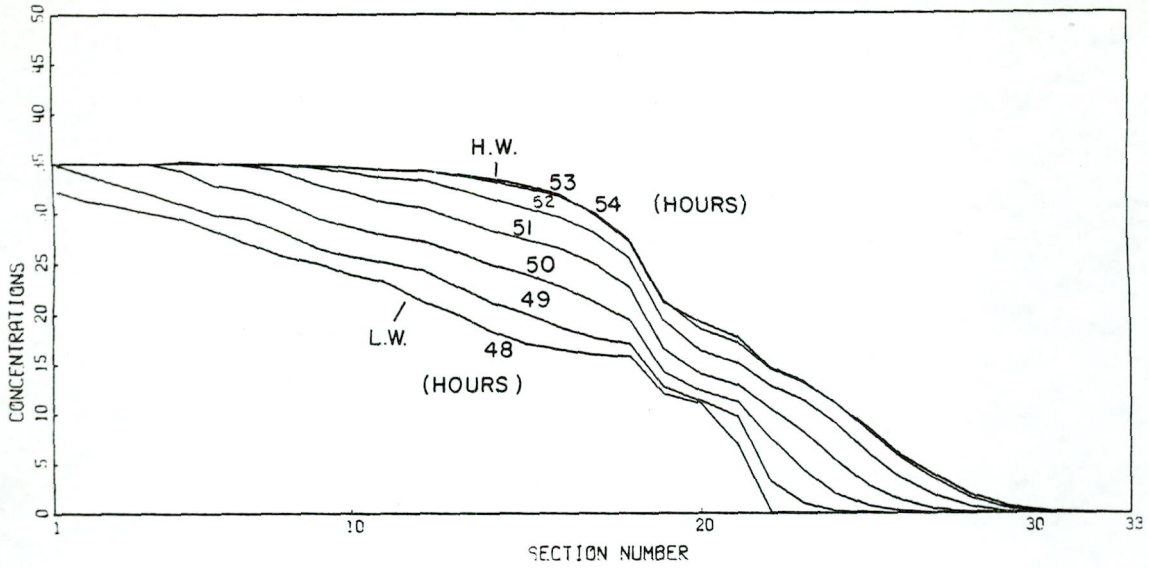

A. SALINITIES AT HOURLY INTERVALS IN MAIN CHANNEL

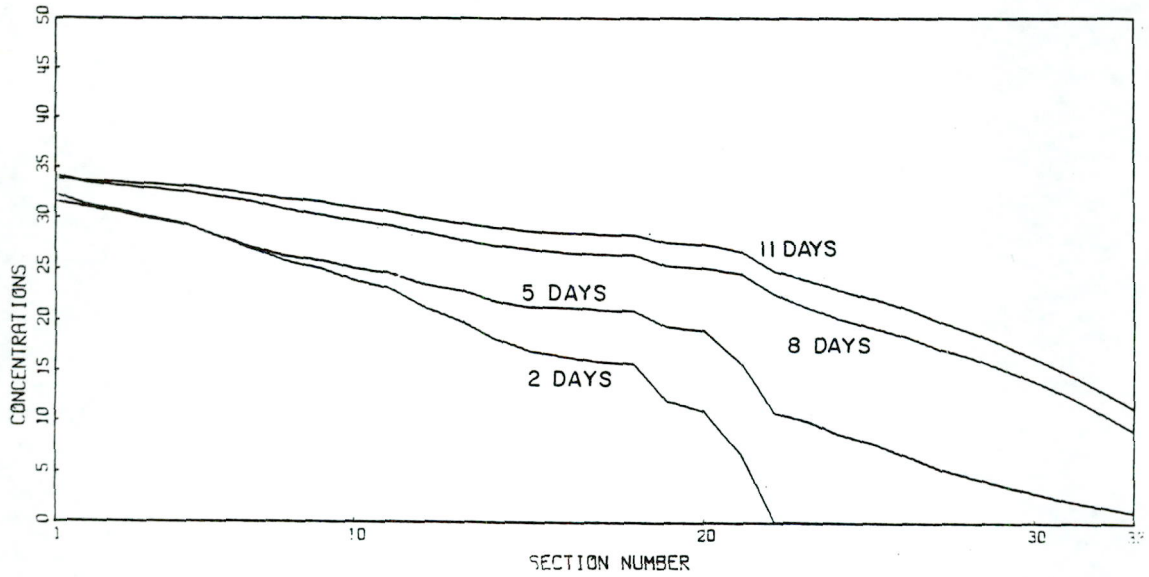

B. SALINITIES AT L.W. AT 3 DAY INTERVALS IN CHANNEL

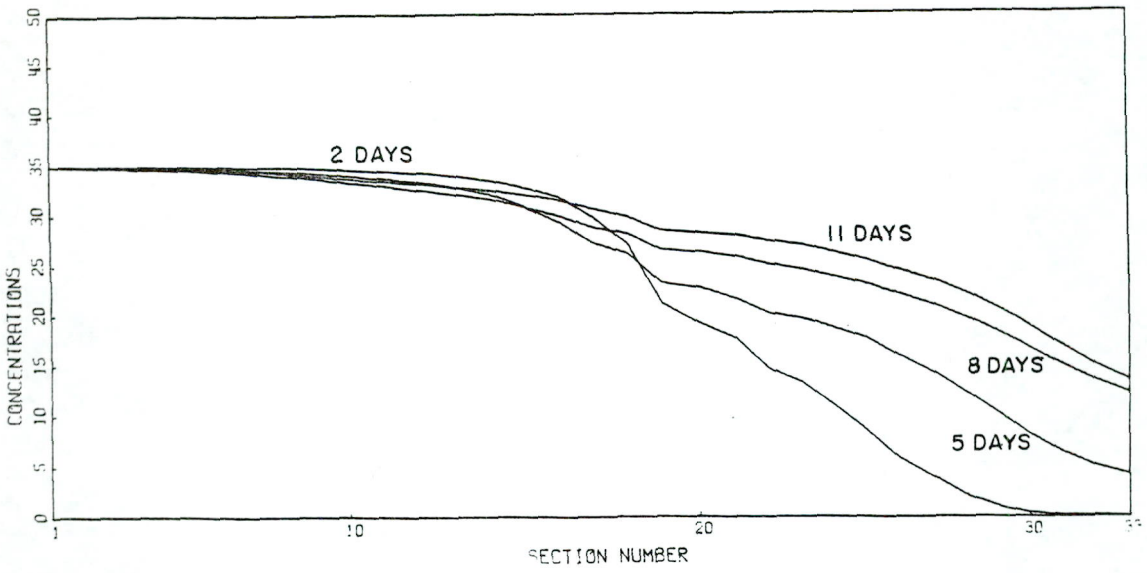

C. SALINITIES AT H.W. AT 3 DAY INTERVALS IN MAIN CHANNEL

TRACED: JGAN CHECKED: DATE: REF.	1 - DIMENSIONAL WATER-QUALITY MODEL KNYSNA MODEL INFLUENCE OF A 1:2 YEAR RIVER FLOOD ON SALINITY CONCENTRATIONS ALONG MAIN CHANNEL AT INDICATED TIMES	FIGURE 28

NATIONAL RESEARCH INSTITUTE FOR OCEANOLOGY

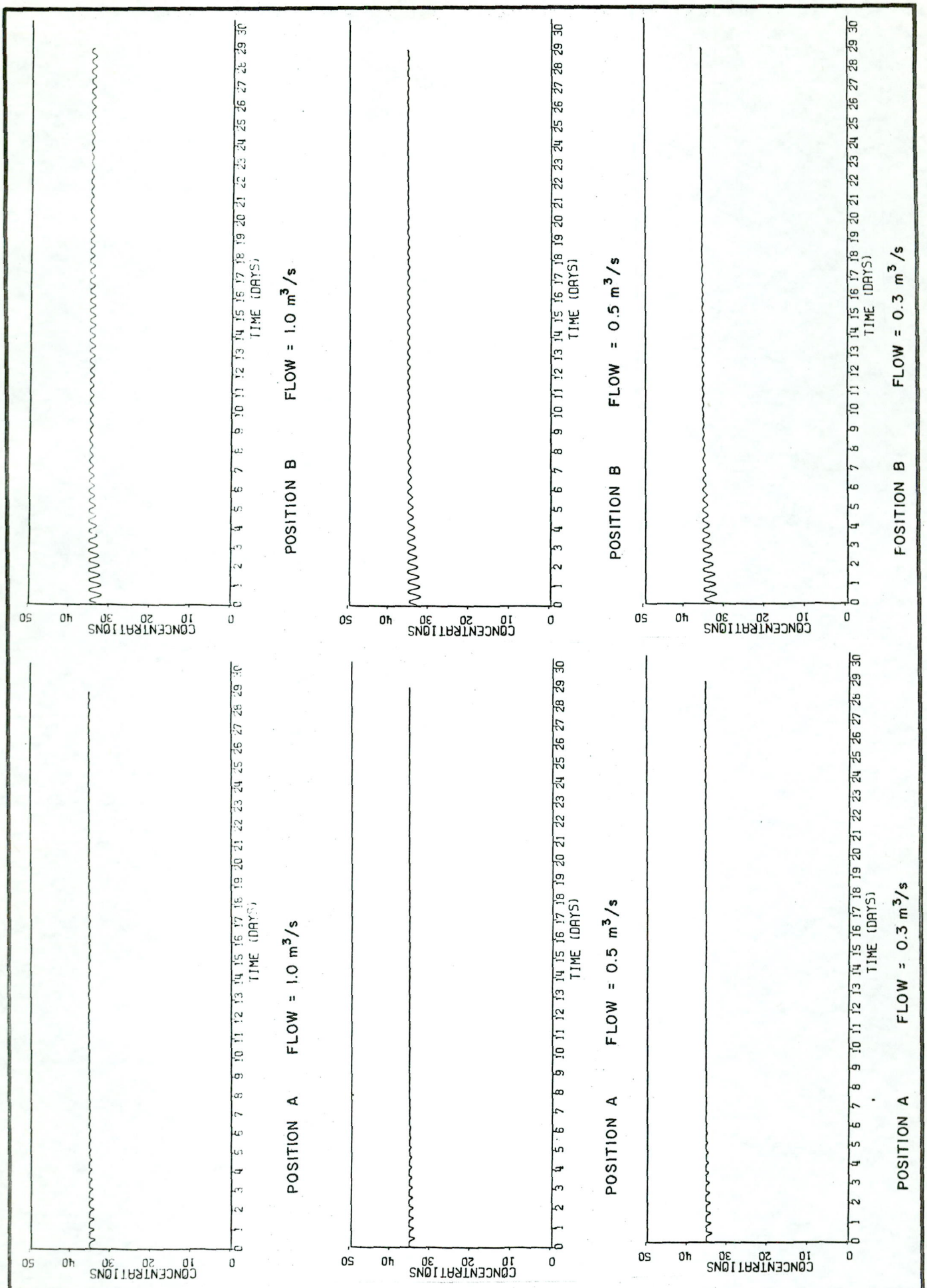

TRACED: JGAN CHECKED: DATE: REF.	1 - DIMENSIONAL WATER-QUALITY MODEL KNYSNA MODEL SALINITIES AT INDICATED POSITIONS UNDER DIFFERENT FLOW CONDITIONS (1.0 ; 0.5 ; 0.3 m^3/s)	FIGURE 29

NATIONAL RESEARCH INSTITUTE FOR OCEANOLOGY

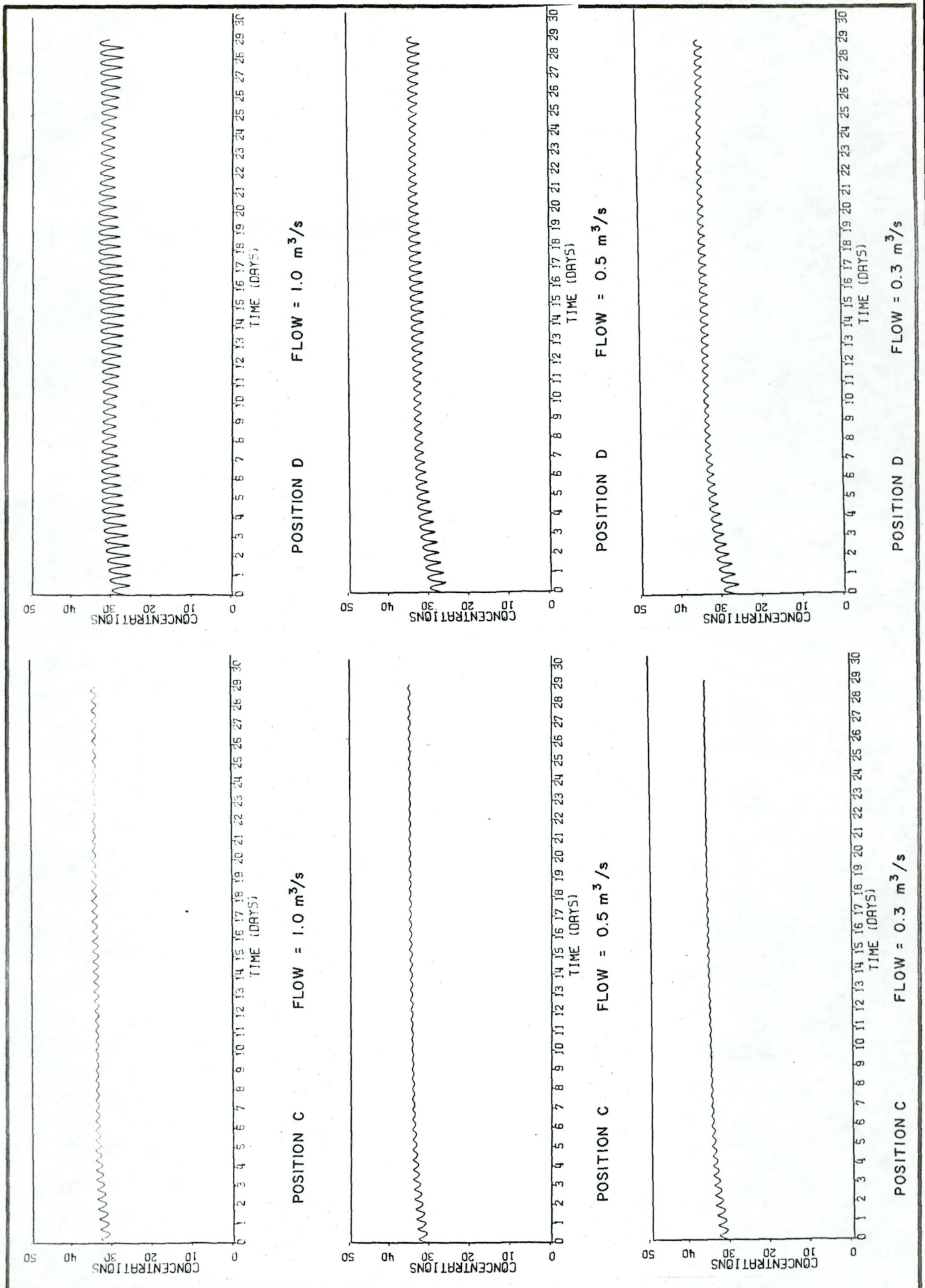

TRACED: JGAN CHECKED: DATE: REF.:	1 - DIMENSIONAL WATER-QUALITY MODEL KNYSNA MODEL SALINITIES AT INDICATED POSITIONS UNDER DIFFERENT FLOW CONDITIONS (1.0; 0.5; 0.3 m^3/s)	FIGURE 30

NATIONAL RESEARCH INSTITUTE FOR OCEANOLOGY

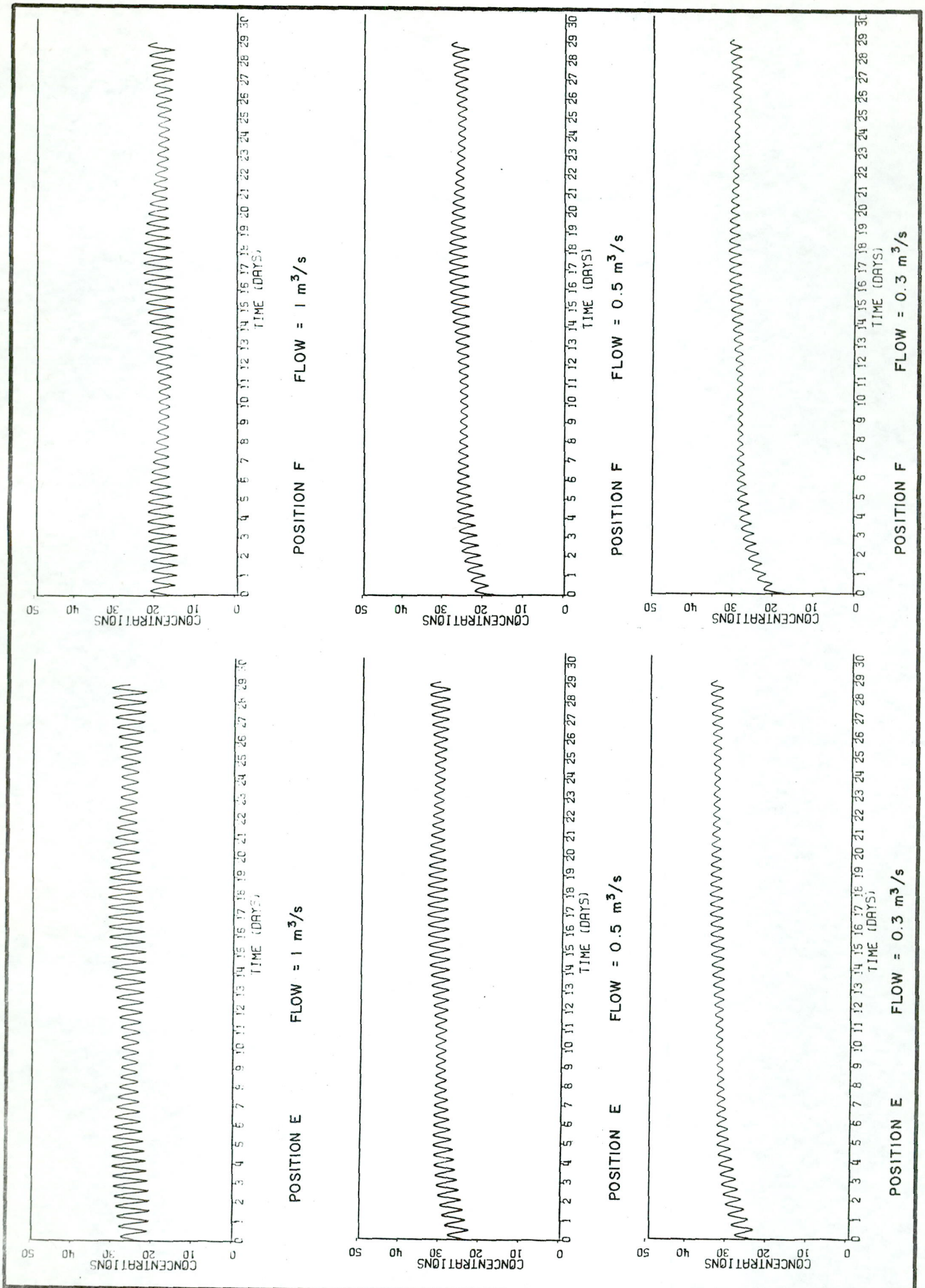

TRACED: JGAN CHECKED: DATE: REF. :	1 - DIMENSIONAL WATER-QUALITY MODEL KNYSNA MODEL SALINITIES AT INDICATED POSITIONS UNDER DIFFERENT FLOW CONDITIONS (1.0 ; 0.5 ; 0.3 m³/s)	FIGURE 31

NATIONAL RESEARCH INSTITUTE FOR OCEANOLOGY

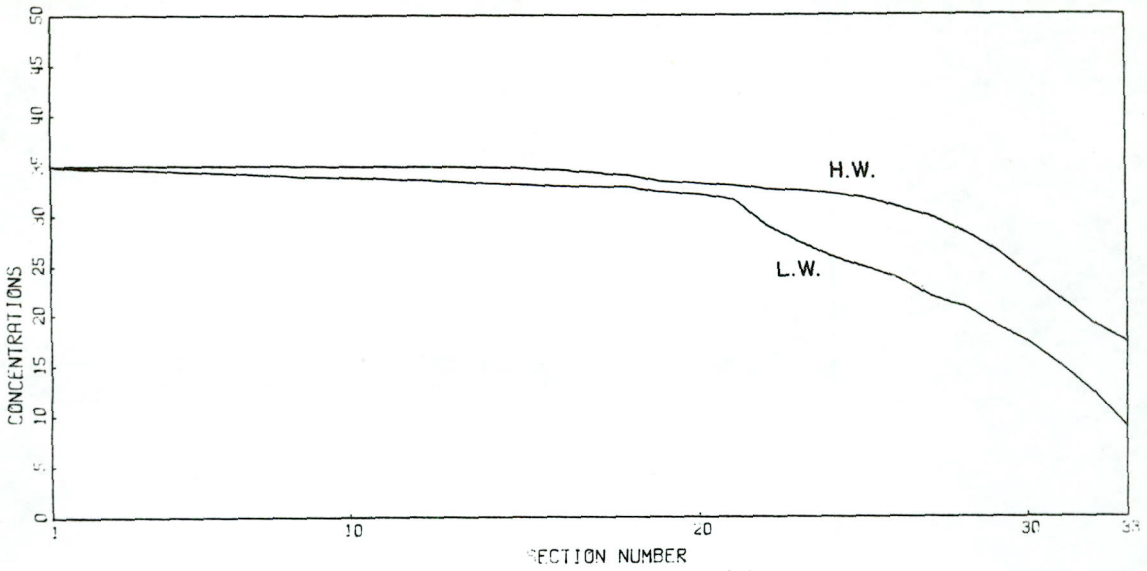

A. SALINITIES AT SPRINGTIDE AND RIVER FLOW OF 1.0 m^3/s

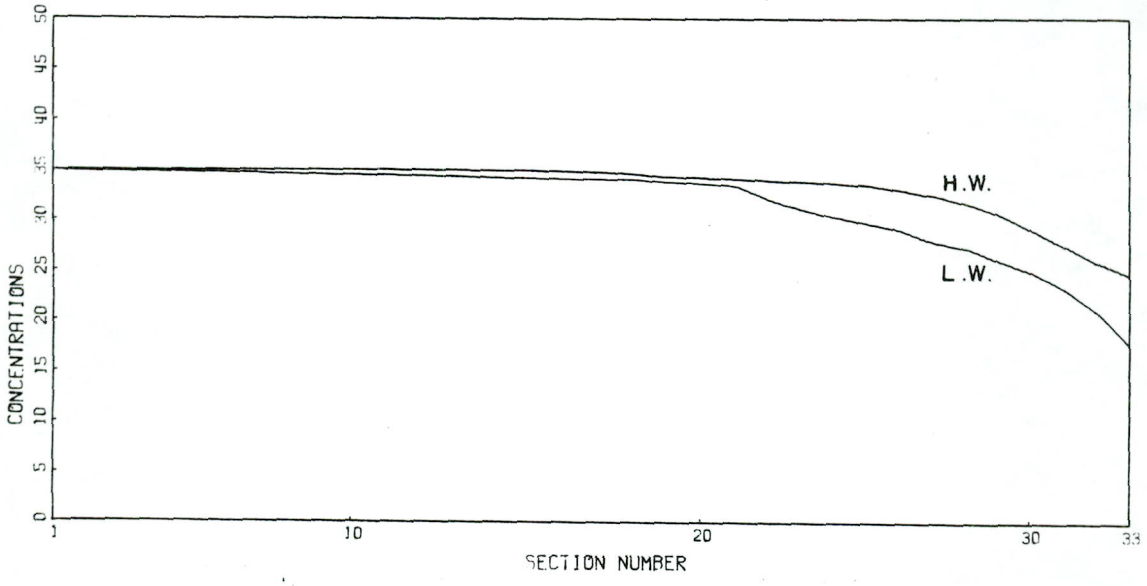

B. SALINITIES AT SPRINGTIDE AND RIVER FLOW OF 0.5 m^3/s

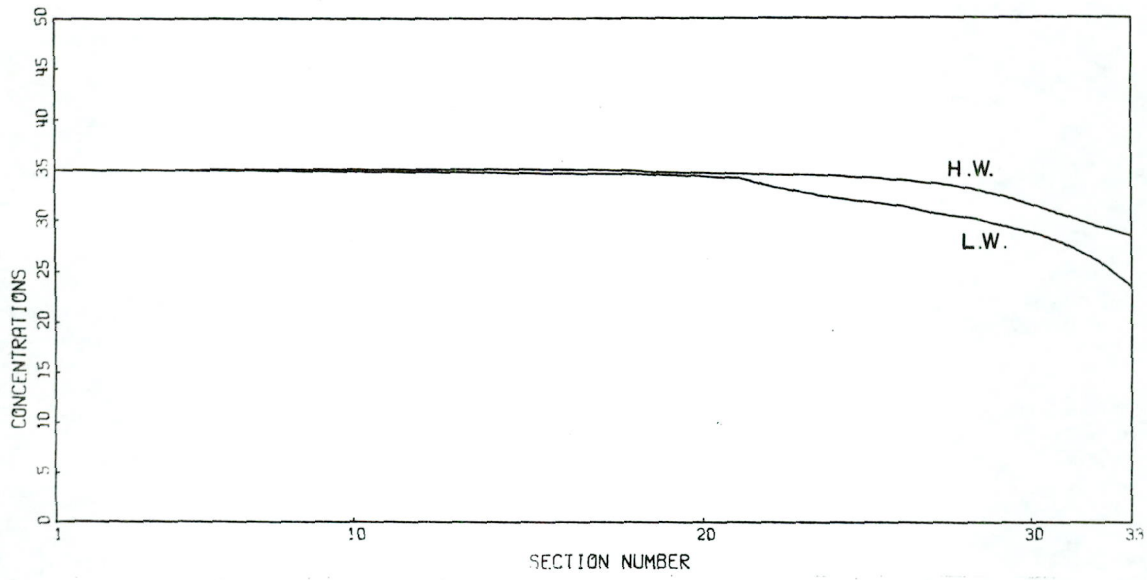

C. SALINITIES AT SPRINGTIDE AND RIVER FLOW OF 0.3 m^3/s

TRACED: JGAN CHECKED: DATE: REF:	1 - DIMENSIONAL WATER-QUALITY MODEL KNYSNA MODEL SALINITIES IN MAIN CHANNEL AT SPRINGTIDE UNDER DIFFERENT FLOW CONDITIONS (1.0 ; 0.5 ; 0.3 m^3/s)	FIGURE 32

NATIONAL RESEARCH INSTITUTE FOR OCEANOLOGY

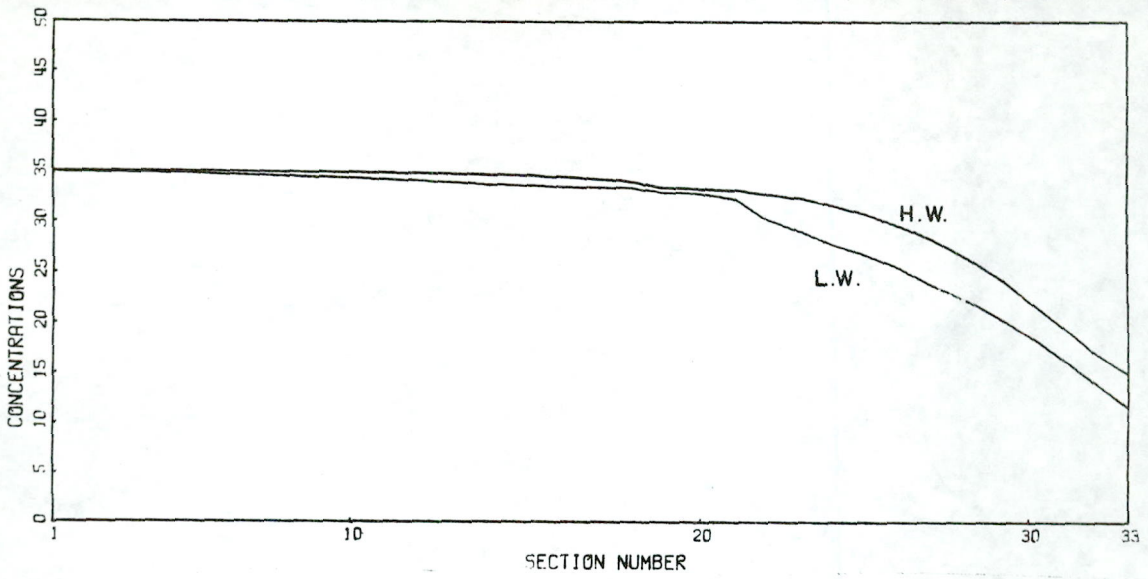

A. SALINITIES AT NEAPTIDE AND RIVER FLOW OF 1.0 m^3/s

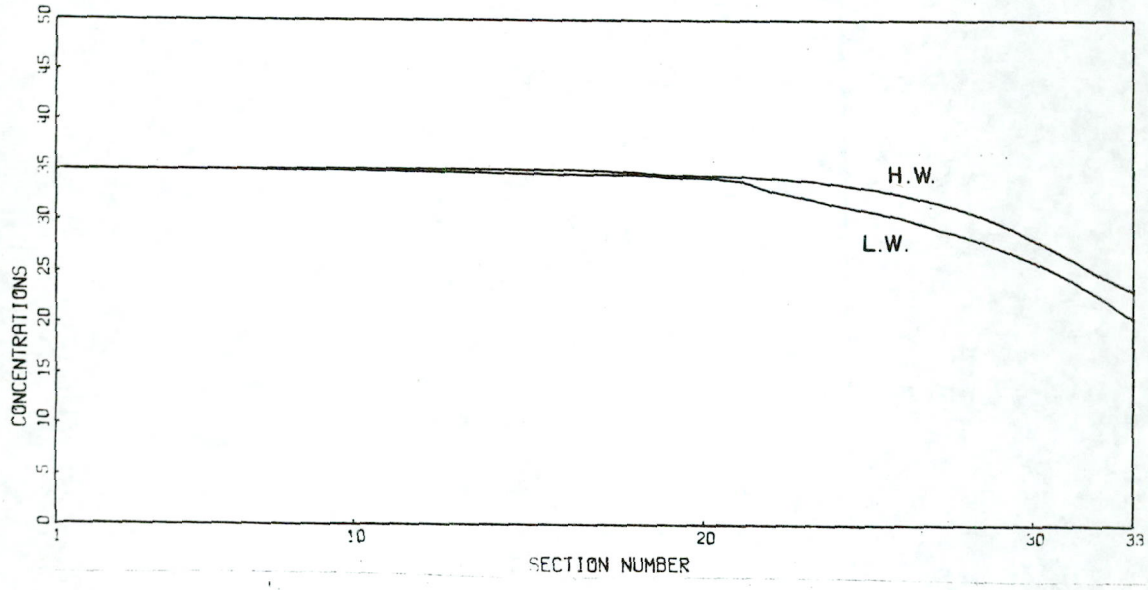

B. SALINITIES AT NEAPTIDE AND RIVER FLOW OF 0.5 m^3/s

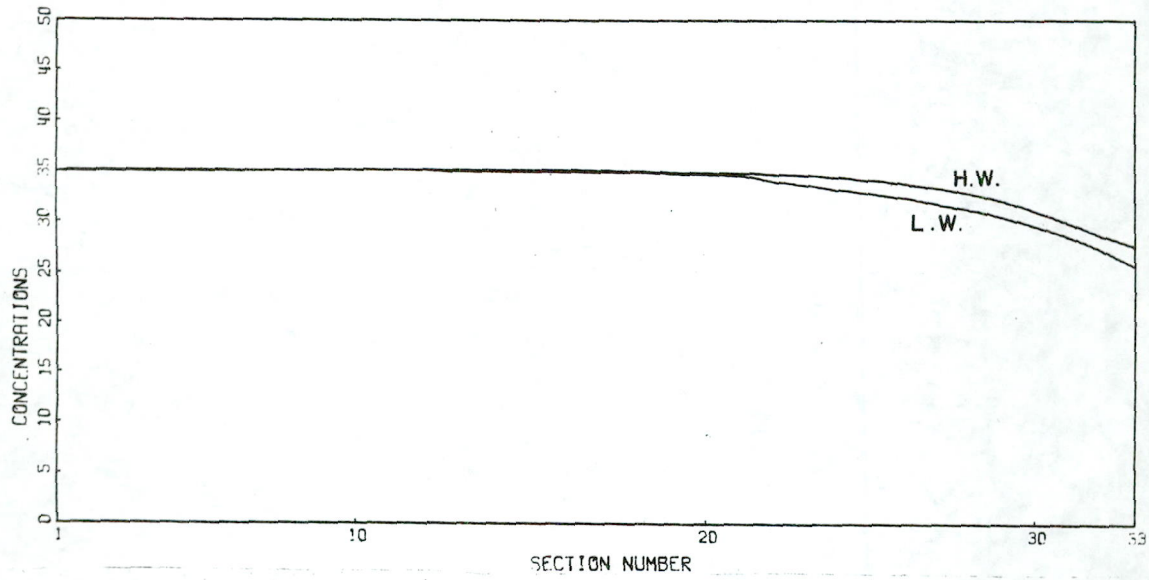

C. SALINITIES AT NEAPTIDE AND RIVER FLOW OF 0.3 m^3/s

TRACED: JGAN CHECKED: DATE: REF.:	1 - DIMENSIONAL WATER-QUALITY MODEL KNYSNA MODEL SALINITIES IN MAIN CHANNEL AT NEAPTIDE UNDER DIFFERENT FLOW CONDITIONS (1.0 ; 0.5 ; 0.3 m^3/s)	FIGURE 33

NATIONAL RESEARCH INSTITUTE FOR OCEANOLOGY